

# **Synthetic Aperture Radar Interferometry (InSAR) Technique**

*(Lecture I- Tuesday 11 May 2010)*

**ISNET/CRTEAN Training Course on Synthetic Aperture Radar (SAR)  
Imagery: Processing, Interpretation and Applications  
3-14 May 2010, Tunis, Tunisia**

*Parviz Tarikhi, PhD*

[parviz\\_tarikhi@hotmail.com](mailto:parviz_tarikhi@hotmail.com)

<http://parviztarikhi.wordpress.com>

**Mahdasht Satellite Receiving Station, ISA, Iran**

- **Rapid and dynamic changes in technologies in recent decades**
- **Space technologies and exploration is avant-garde**
- **Sensing and detecting phenomena from long distance is of great importance and effect.**
- **Electromagnetic waves the tool for long range sensing of the phenomena**
- **Radar Remote Sensing an effective mean that uses  
Electromagnetic waves characteristics for SAR  
Interferometry**



**Synthetic Aperture Radar (SAR) technology is an efficient tool for monitoring and investigation of dynamic phenomena on Earth.**

# OUTLINE

- **Introduction**
- **Use of interferometric products**
- **INSAR System components**
- **Historical review**
- **SAR systems**
- **INSAR software**
- **Consumer market of applications**
- **Future Trends**
- **Electromagnetic Radiation & Interference Concepts**
- **InSAR Technique and Principles**
- **Data Investigation**
- **Information Analysis**

## Introduction

- Interferometric Synthetic Aperture Radar  
(INSAR or IFSAR)

*a technique for extracting topographic and thematic information  
using the **wave characteristics** of radar signals*

- SAR phase data

*generating phase difference images from two or more (repeat pass)  
data collections*

*The images called interferogram*

- Coherence maps,

*a measure of the equality of two SAR datasets, can be generated*

## Use of interferometric products

### *Digital Elevation Models (DEM) or Digital Terrain Models (DTM)*

created using the interferogram of two SAR datasets acquired at slightly different sensors positions

### *Deformation maps*

created using a technique called Differential InSAR (DInSAR)

*calculates* the difference between two interferograms belonging to three datasets acquired at different moments

*applied* to detect positional changes on the earth surface caused by ice flows, tectonic plates shifts or volcanic movements, ...

*between the acquisitions of three or more SAR datasets*

### *Thematic maps*

created using coherence maps

*degree* of coherence is related to the stability of the chemical and structural composition of the groundcover between the moments of the data acquisition

- *different vegetation type can have different coherence.*

## InSAR System components

- To generate DTM's, deformation maps or thematic maps,  
*two or more SAR datasets of the same area acquired by the same sensor systems  
are necessary*  
*datasets are in such a format that they still contain the phase and magnitude  
information of the radar signal and also the orbit, timing, calibration and other  
essential parameters of these data are available*
- To produce a DTM  
*a software package containing the below functionalities needed*

**Data input**

**Coregistration of the data sets**

**Coherence map generation**

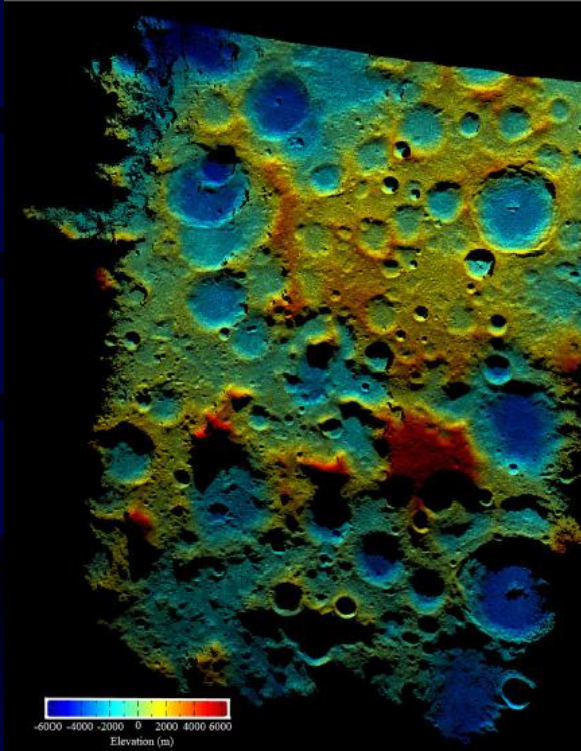
**Interferogram generation**

**Phase unwrapping**

**DTM generation**

## Historical review

- 1969: InSAR used for the first time in observation of the surface of Venus and the Moon by Rogers and Igalis



*High-resolution topographic map of the Moon generated by SAR*

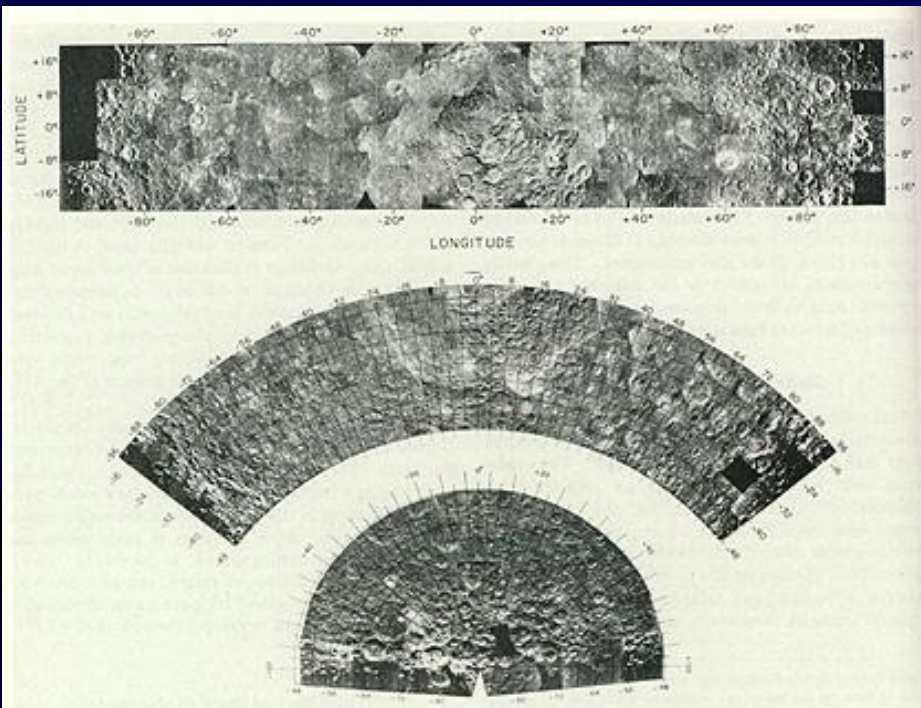
*The surface of Venus, as imaged by the Magellan probe using SAR >*





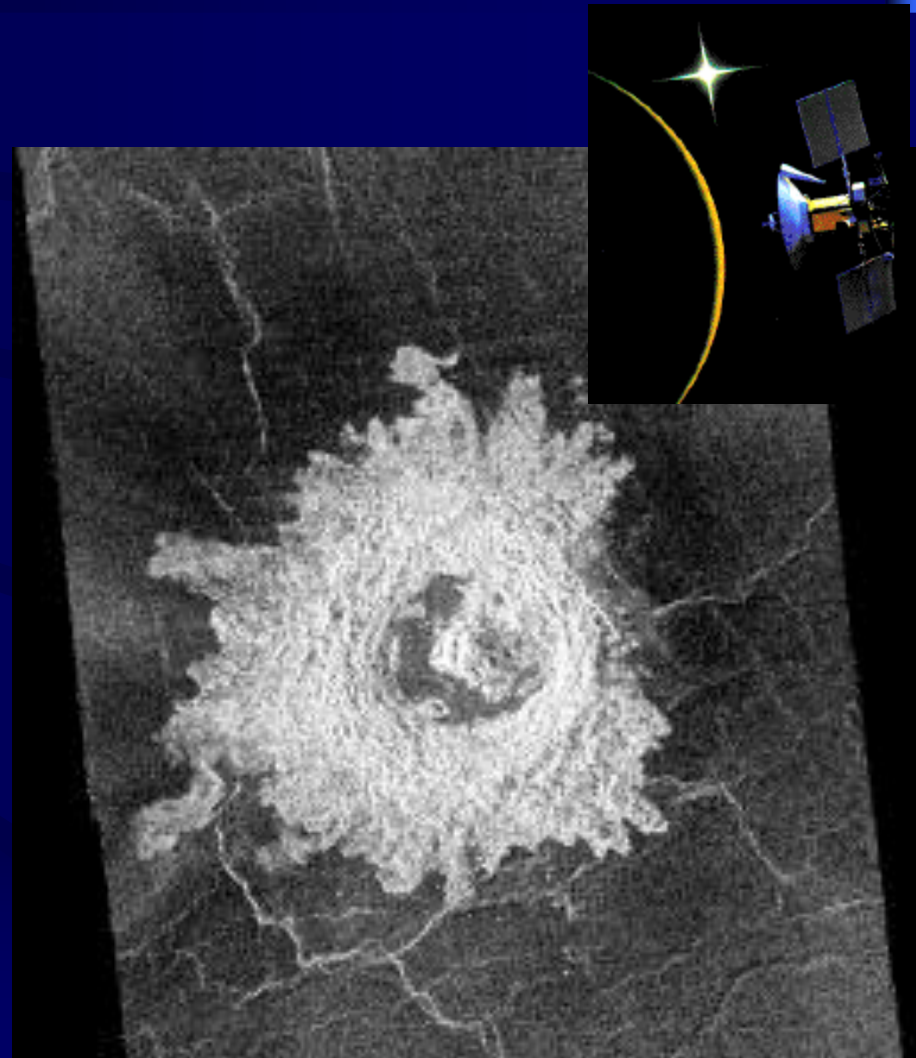
# Historical review (continued)

## Observing the surface of Venus and the Moon by InSAR



*Topographic map of the Moon generated by SAR*

*The surface of Venus, imaged by SAR >*



## Historical review (continued)

- 1974: Graham was the first to introduce SAR for topographic mapping

There are two kinds of information that are acquired for the production of topographic maps.

*Firstly*, the various objects and features to be mapped must be present in the image with sufficient resolution to be identified.

*Secondly*, a three-dimensional measurement of the position, with respect to the sensor platform, of a sufficient number of points must be executed to define the terrain surface.

These measurements can be realized by means of InSAR with SAR data that is collected by sensors on airborne or spaceborne platforms.

- 1985: Zebker and Goldstein started a research at Jet Propulsion Laboratory (JPL) in Pasadena, California. They mounted two SAR antennas on an aircraft with a distance (the baseline) of 11.1 m from each other. Both antennas received the signals transmitted from one antenna simultaneously.

## Historical review (continued)

- 1988: Goldstein transferred the concept of the airborne images to the SEASAT data

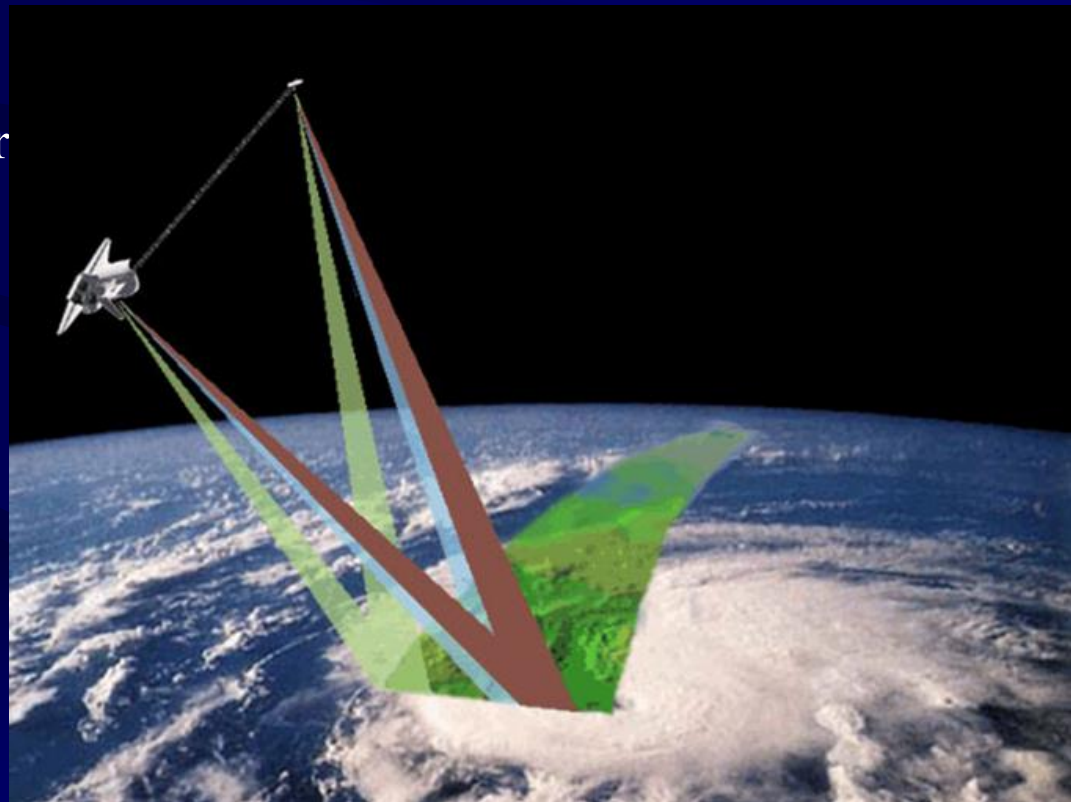
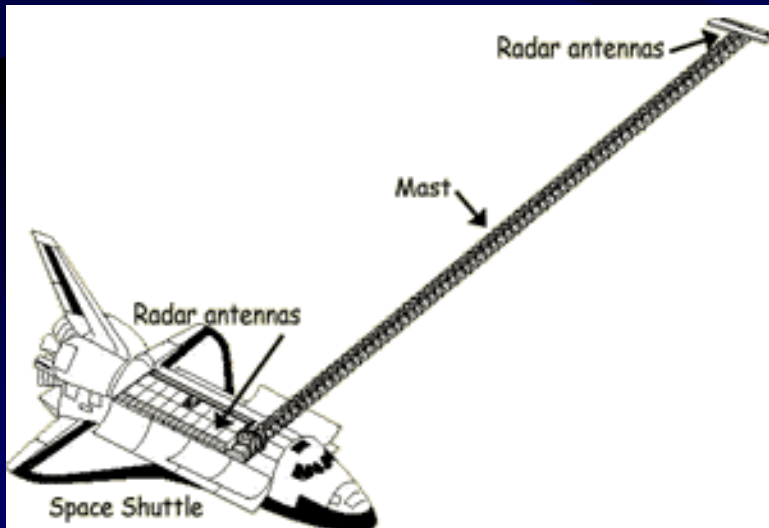


SEASAT, USA

## Historical review (continued)

- 1988: Gabriel and Goldstein adapted the InSAR technique to the space shuttle mission that collected the SIR-B radar data

SRTM (Shuttle Radar Topography Mission)/ 2000/ Endeavour



## Historical review (continued)

- 1991: European Space Agency (ESA) launched the ERS-1 satellite with its C-band SAR;
- 1995: ERS-2 is launched. After its launch the opportunities for spaceborne InSAR were extended using ERS-1 and ERS-2 in tandem mode (radar data acquisition only one day apart)
- 1995: Canadian RADARSAT satellite launched successfully and data from that system became available to extract topographic information by means of InSAR
- 2002: ESA's Envisat is launched
- 2006: Japanese ALOS is launched
- 2008: German TerraSAR-X is launched

# SAR systems

SAR systems installed on spaceborne and airborne platforms

## Imaging RADAR Systems

- **Airborne**

Emisar : C, L band, University of Denmark, Denmark

AeS-1: X, P band Aerosensing, Germany

Pharus: C band FEL-TNO, Netherlands

Star-31: X band Intermap, Canada

Airsar/topsar: P, L, C band, NASA/JPL, USA

Carabas: 3-15cm, Chalmers University/FOI, Sweden

Geosar: X, P band, JPL and others, USA

WINSAR: 4 bands, Metratec, USA

## **SAR systems (continued)**

SAR systems installed on spaceborne and airborne platforms

### **Imaging RADAR Systems**

#### **Spaceborne**

ERS-1: C band (Not operational anymore), ESA

JERS-1: L band (Not operational anymore), Japan

ERS-2: C band, ESA

Radarsat: C band, Canada

SRTM: C and X band, Space shuttle mission, NASA, USA

Envisat: C band, ESA

ALOS: L band, Japan

TerraSAR-X, X band, Germany

# SAR systems (continued)

## Spaceborne Imaging RADAR Systems

### InSAR Satellites



ERS

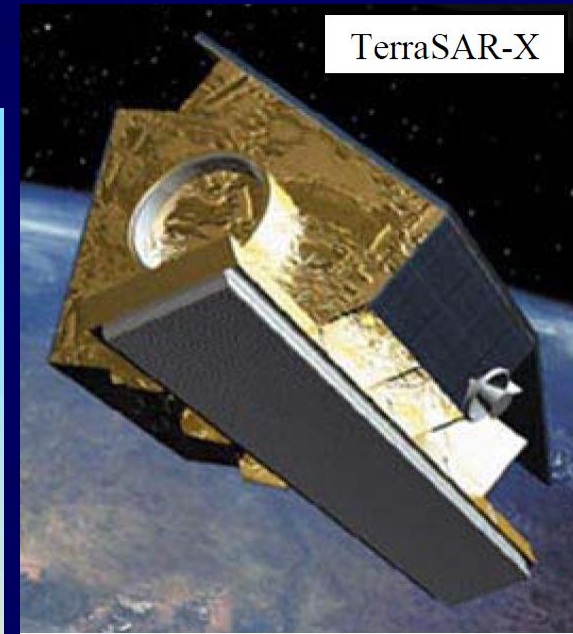


Envisat

ALOS



Radarsat



TerraSAR-X

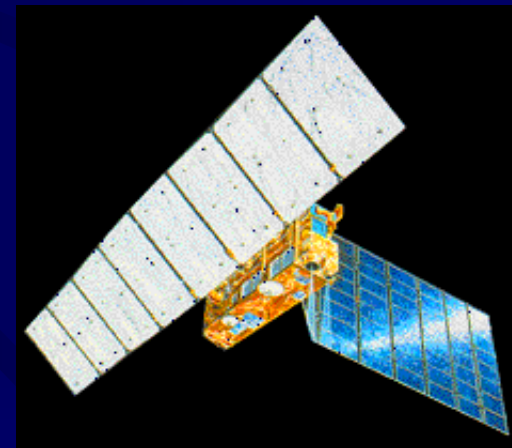


RADARSAT-2



## SAR systems (continued)

- The first and second European Remote Sensing (ERS) satellites are the earliest orbiting platforms which their data have been applied for SAR Interferometry.
- ERS-1 and ERS-2 launched in 1991 and 1995. European Space Agency (ESA) operates these satellites.
- Canadian Radarsat-1 equipped with imaging radar was launched in 1995.
- The first Japanese Earth Resource Satellite (JERS-1) was orbited two years earlier in 1992.



# SAR systems (continued)

## Platforms of Spaceborne Imaging RADAR Systems

### InSAR Platforms

<b>Major SAR Sensors</b>						
<b>Characteristics/Satellite</b>	ERS* 1/2	JERS**	Radarsat	Envisat	ALOS***	TerraSAR-X
<b>Operator</b>	ESA	Japan	Canada	ESA	Japan	Germany
<b>Time coverage</b>	1991-2004/ 1995-	1992-1998	1995-	2002-	2006-	2007-
<b>Wavelength</b>	C-band (6cm)	L-band (24cm)	C-band	C-band	L-band	X-band (3cm)
<b>Orbit repeat</b>	35 days	44 days	24 days	35 days	46 days	11 days

\*ERS: European Remote Sensing Satellite

\*\*JERS: Japanese Earth Resources Satellite

\*\*\*ALOS: Advanced Land Observation Satellite – Daichi

## INSAR software

There are several software packages that can process SAR data into interferometric products for many applications.

### The list of common InSAR software packages

- **EPSIE 2000** , Indra Espacio, Spain
- **DIOPSON**, French Space Agency (CNES)/Altamira Information, France
- **ERDAS Imagine** (ERDAS InSAR), Leica Geosystems, USA
- **Earth-View (EV) InSAR**, Atlantis Scientific Inc. of Canada/USA
- **GAMMA**, GAMMA Remote Sensing and Consulting AG, Switzerland
- **ROI PAC**, NASA's Jet Propulsion Laboratory and CalTech., USA
- **SARscape**, ENVI, Germany
- **PulSAR and DRAIN**, Phoenix Systems Ltd., UK
- **SAR-E2**, JAXA, Japan (developed for JERS SAR data examining)
- **DORIS**, Delft University of Technology, The Netherlands, (*Delft Object-oriented Radar Interferometer Software*)

SAR Toolbox, BEST (Basic Envisat SAR Toolbox), NEST (Next ESA SAR Toolbox)

## Consumer market of applications

Spaceborne SAR interferometry holds great promise as a change-detection tool in the fields of

- earthquake studies,
- volcano monitoring,
- land subsidence detection, and
- glacier and ice-stream flow studies.

other fields includes

- hydrology,
- geo-morphology,
- ecosystem studies

The market for Airborne interferometric products is the same as for the laser altimetry.

# The future

- The trend in airborne InSAR is towards  
multi frequency and multi polarization systems
- The advantages of a long-wave-band (L or P) are that they can penetrate canopy and will probably result in a ground surface height map in dense forest.
- The use of combinations of short-wave-bands (X or C) with long wave band will enable bio mass estimation.
- use of multi polarization InSAR enables the creation of optimized interferograms applying a weighted contribution of the different polarizations (HH, HV, VV).
- The usage of airborne SAR sensors for differential interferometry is of great interest.
- usage of longer wavelengths with better coherence behavior, like L-or P-band, offers the possibility of an analysis of long-term processes even in case of vegetated areas.
- the capabilities for monitoring of short-term processes is improved by the greater flexibility of airborne sensors.
- Particularly, the combination of operationally generated space-borne interferometric SAR data with flexibly acquired airborne data seems to be very promising
- The future in spaceborne interferometry will be mainly in the direction of Differential InSAR for several applications where change detection is important.

# Electromagnetic Radiation & Interference

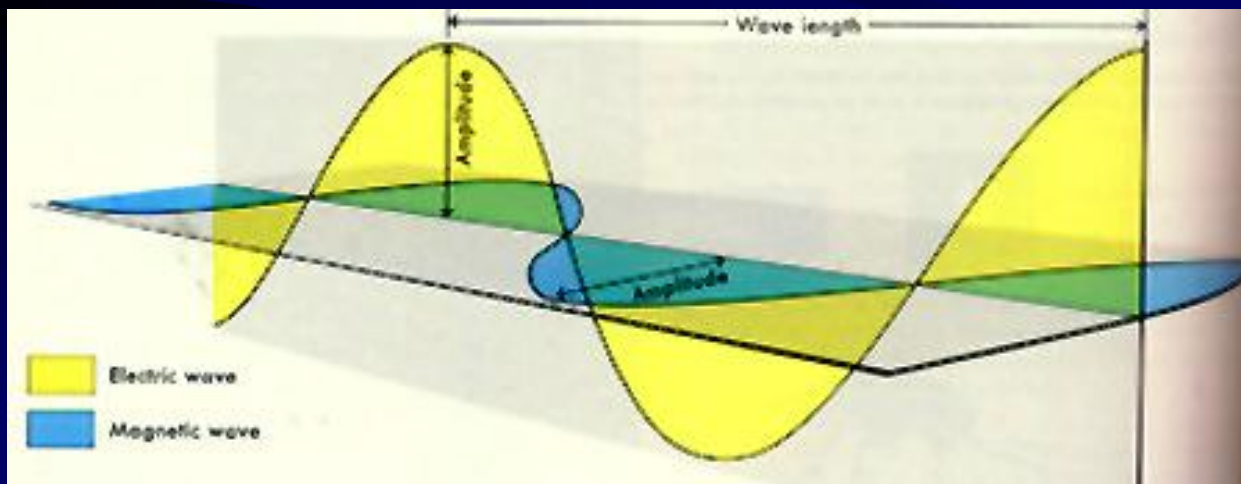
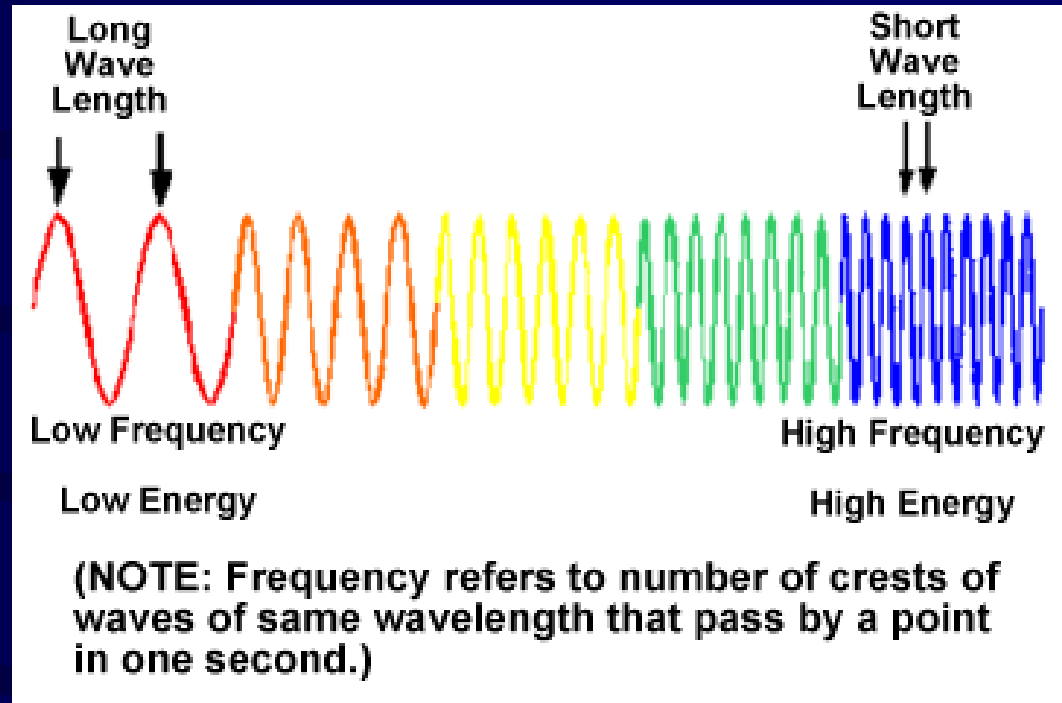
*Concepts*

# The Electromagnetic Spectrum and Energy

## The Photon

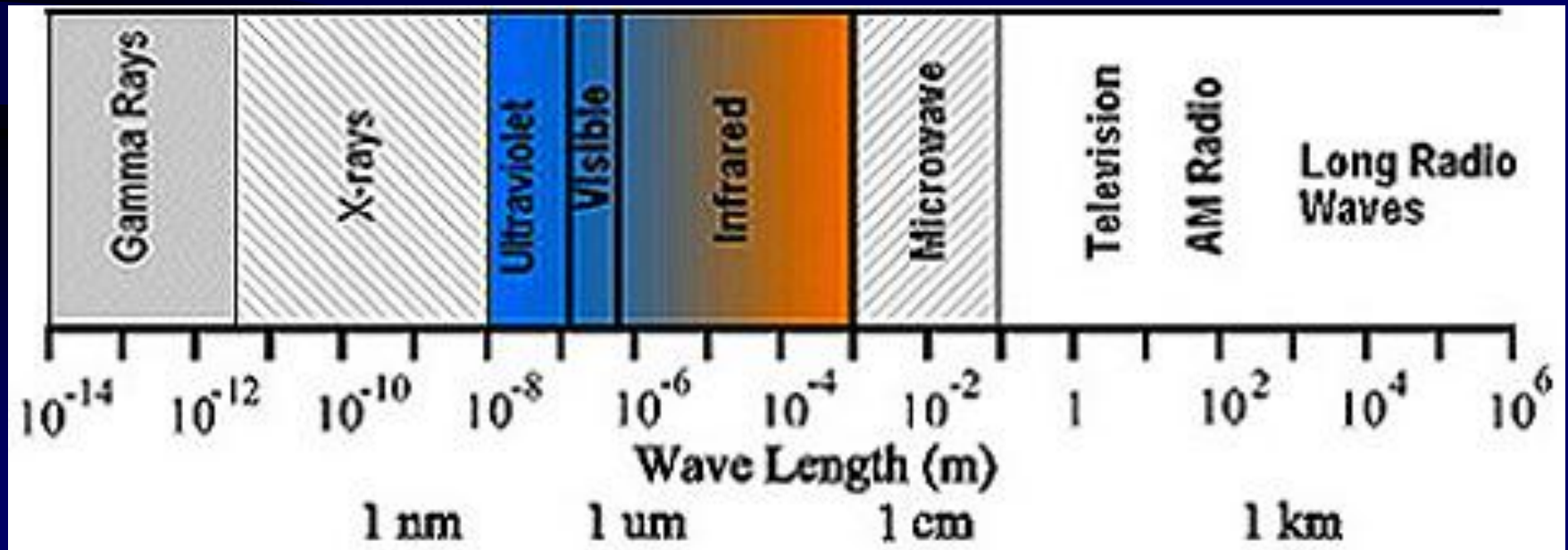
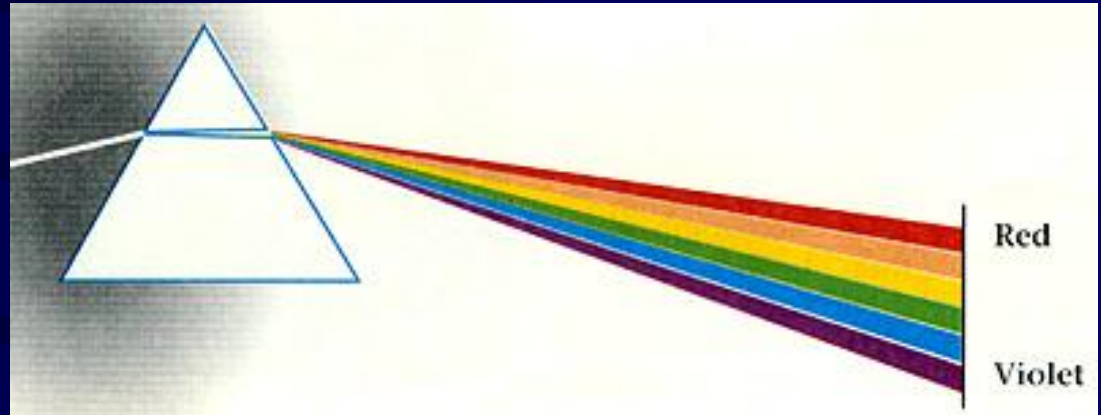
*A pack of electromagnetic energy localized in space and time*

*Electromagnetic wave*



# The Electromagnetic Spectrum and Energy

*Electromagnetic Spectrum: Distribution of Radiant Energies*

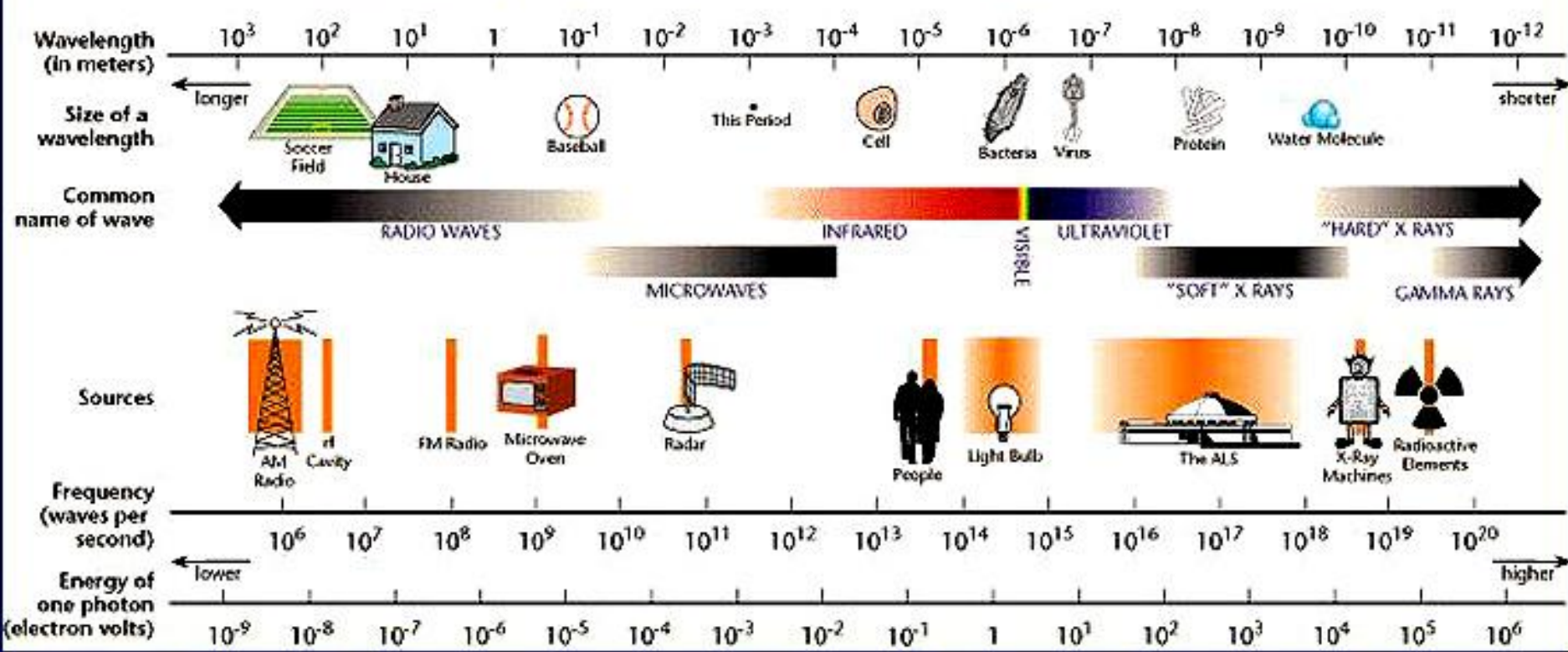




# The Electromagnetic Spectrum and Energy

*Electromagnetic Spectrum: Distribution of Radiant Energies*

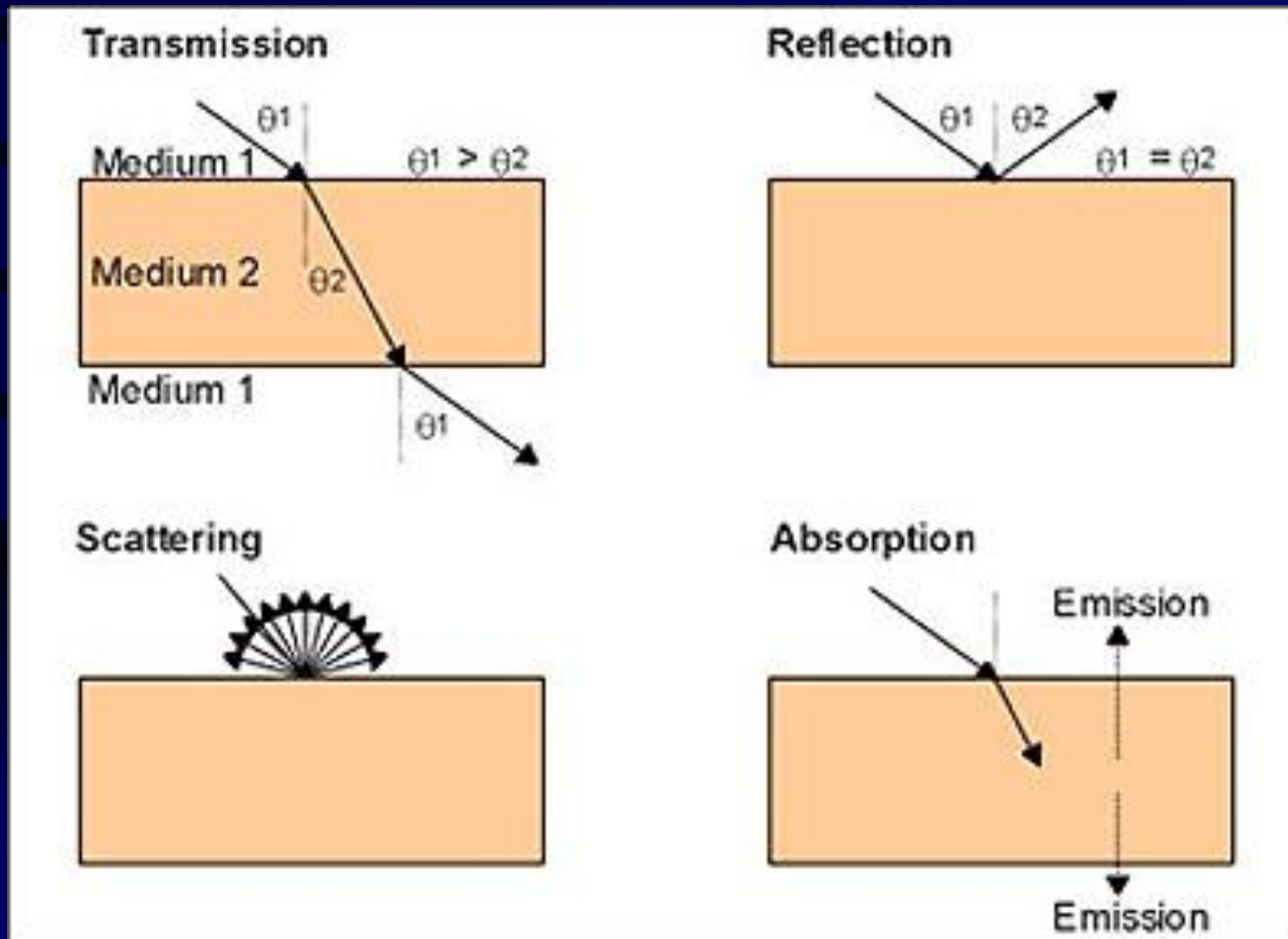
## THE ELECTROMAGNETIC SPECTRUM



# The Electromagnetic Spectrum and Energy

Transmission, Absorption, Reflectance and Scattering

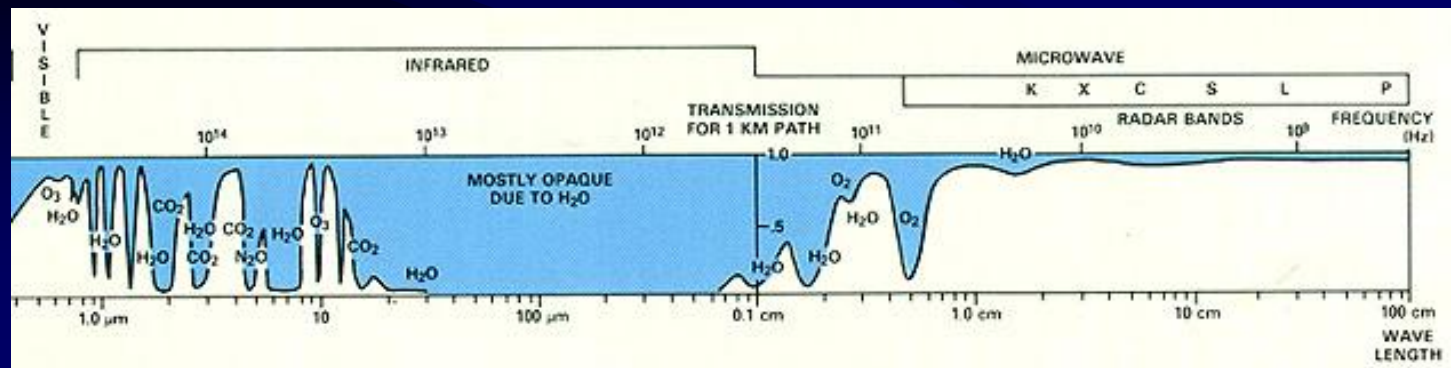
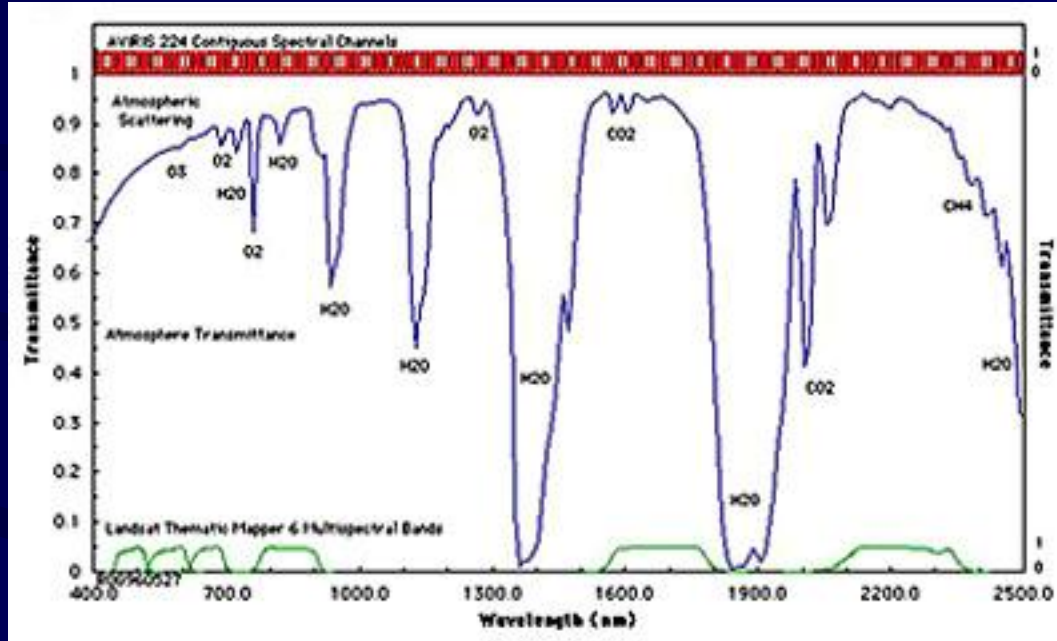
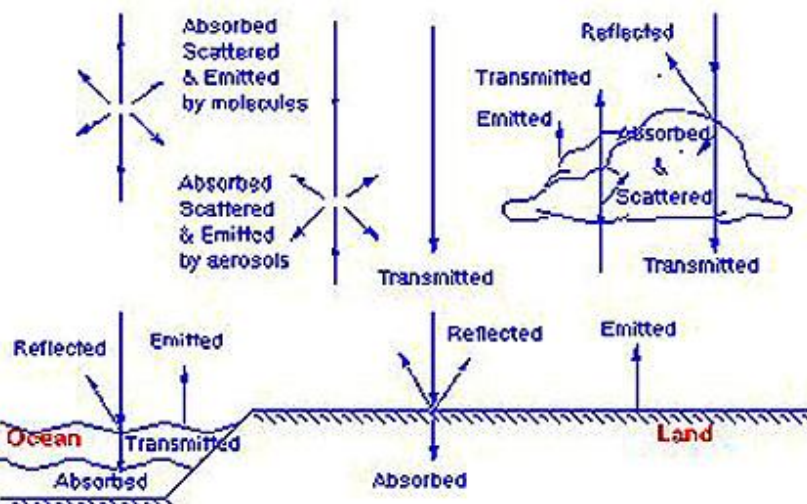
*The concept and model*



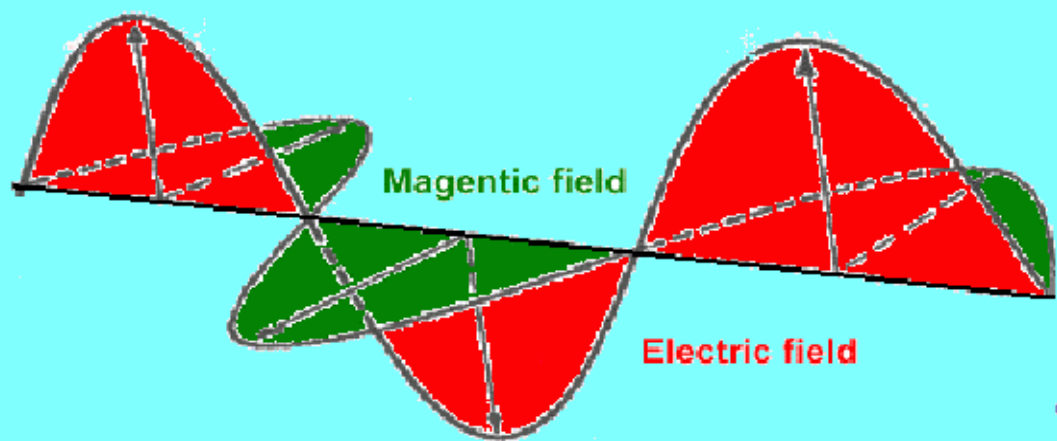
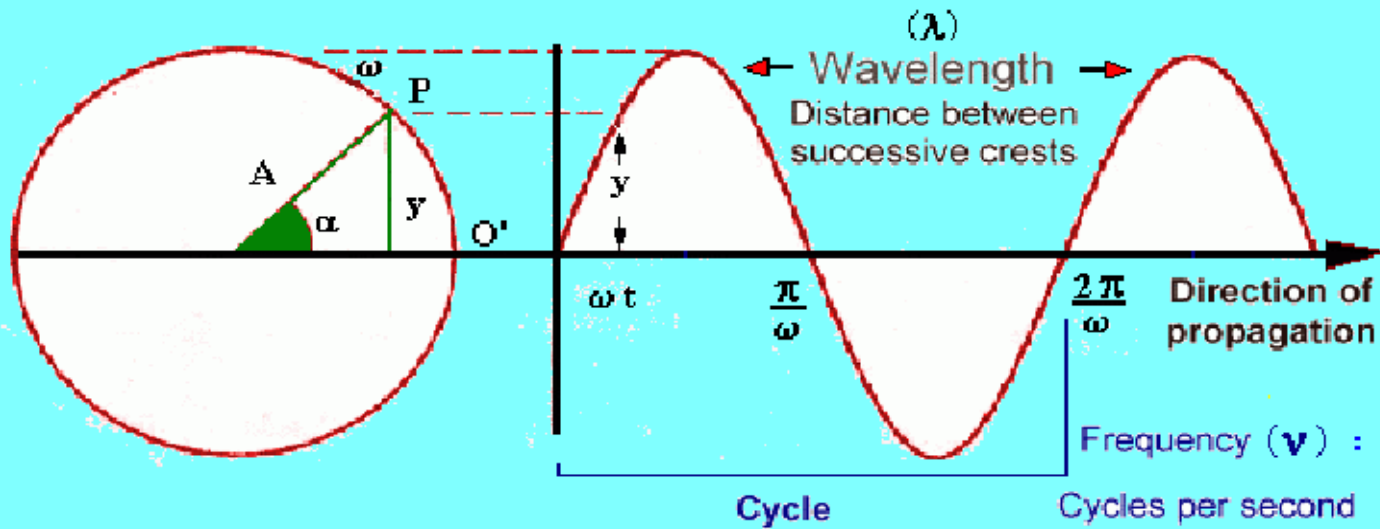
# The Electromagnetic Spectrum and Energy

Transmission, Absorption, Reflectance and Scattering  
*Electromagnetic Spectrum: Distribution of Radiant Energies*

Processes of Atmospheric Radiation



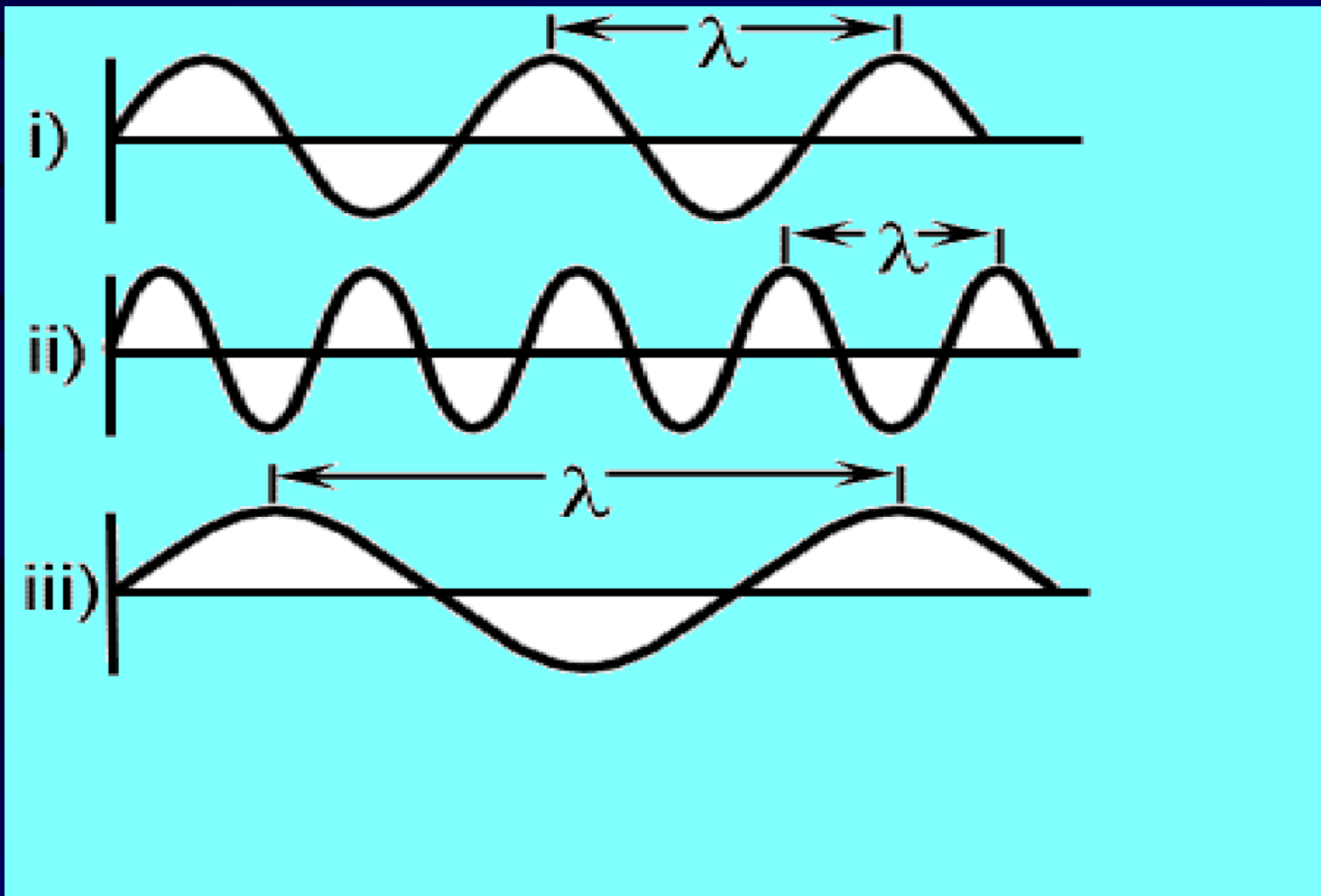
# Electromagnetic Waves



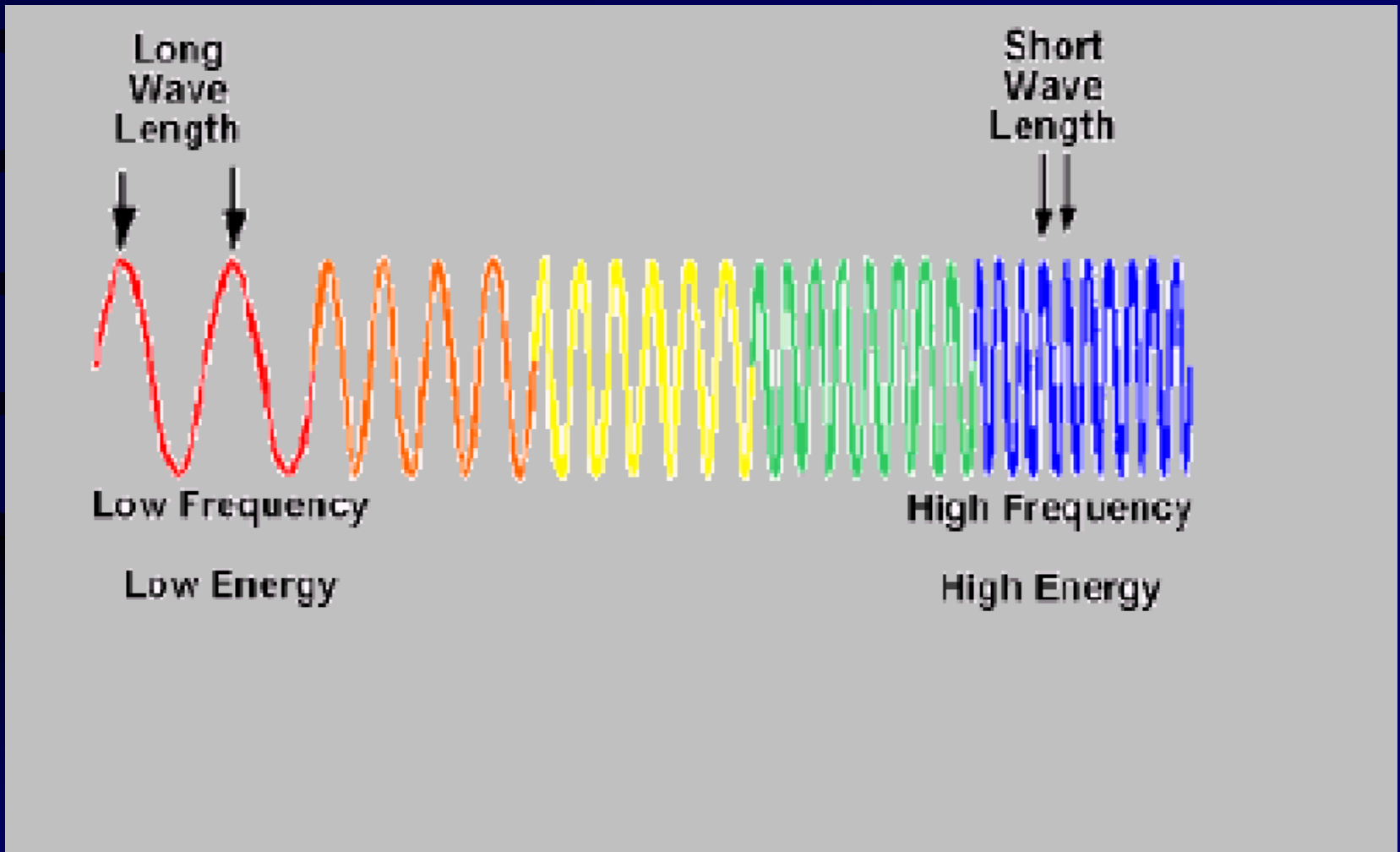
$$\lambda \cdot \nu = c$$

$$\frac{\text{metres}}{\text{cycles}} \cdot \frac{\text{cycles}}{\text{seconds}} = \frac{\text{metres}}{\text{seconds}}$$

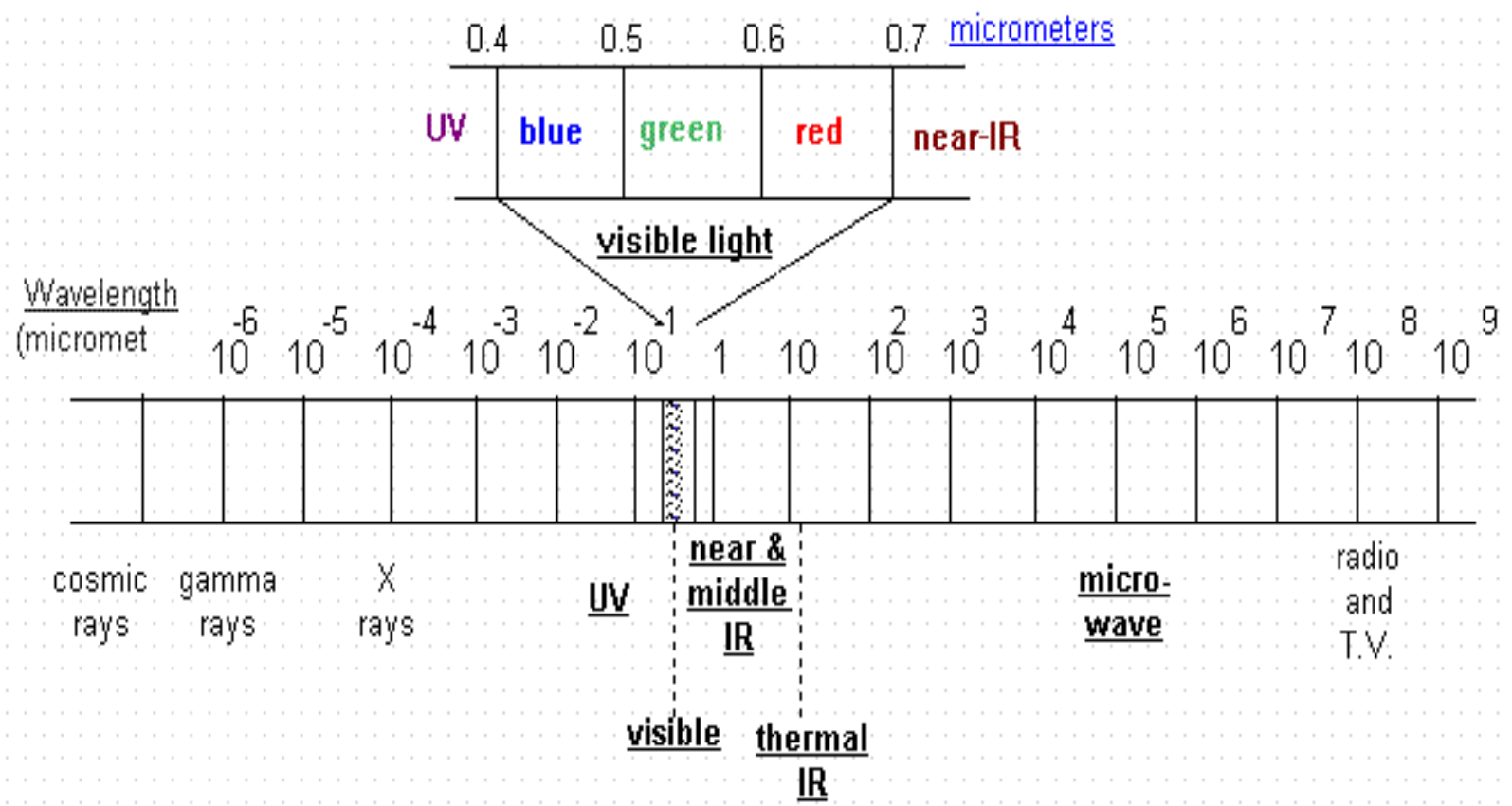
# Wavelength and Frequency



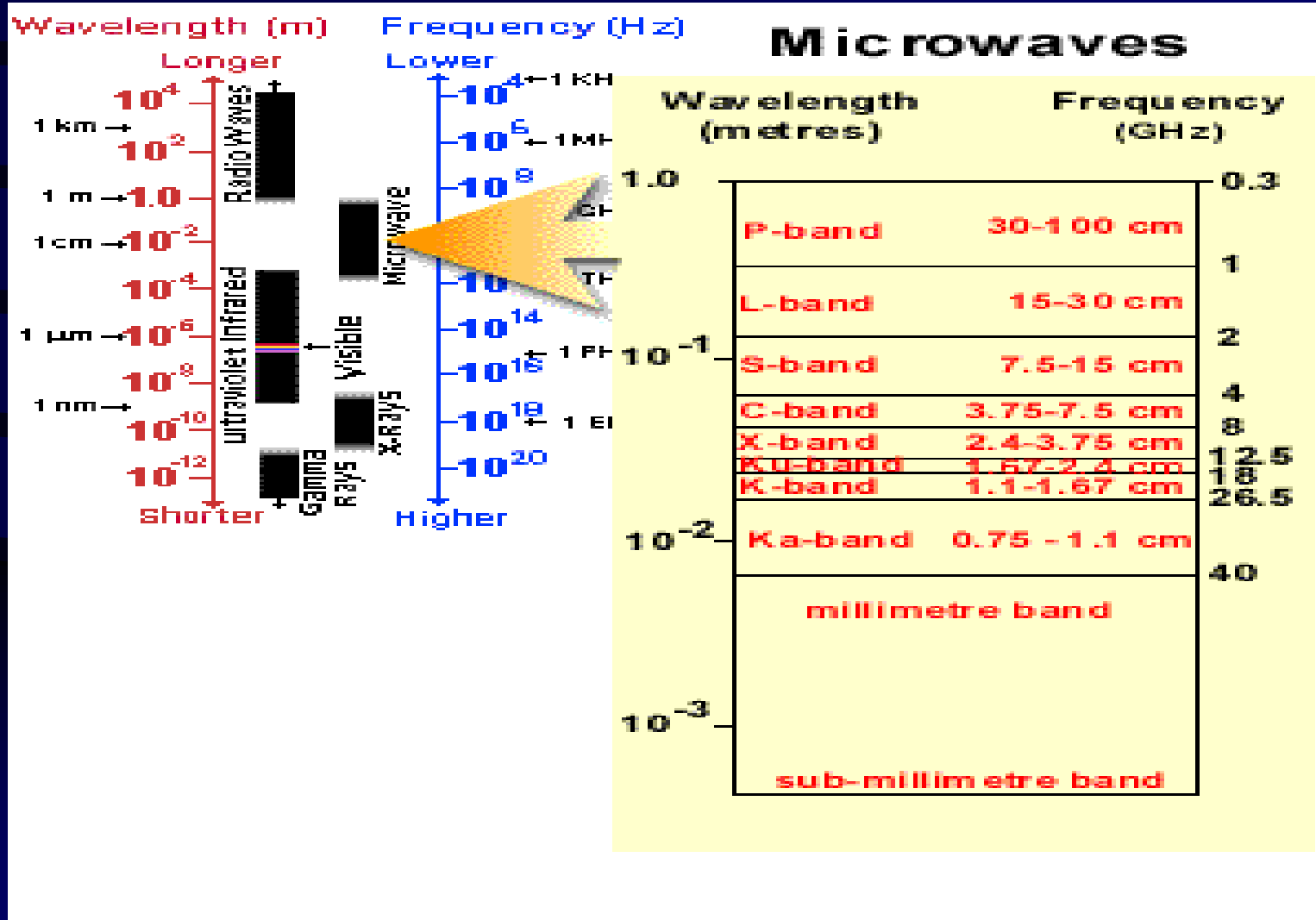
# Visible Frequency



# The Electromagnetic Spectrum

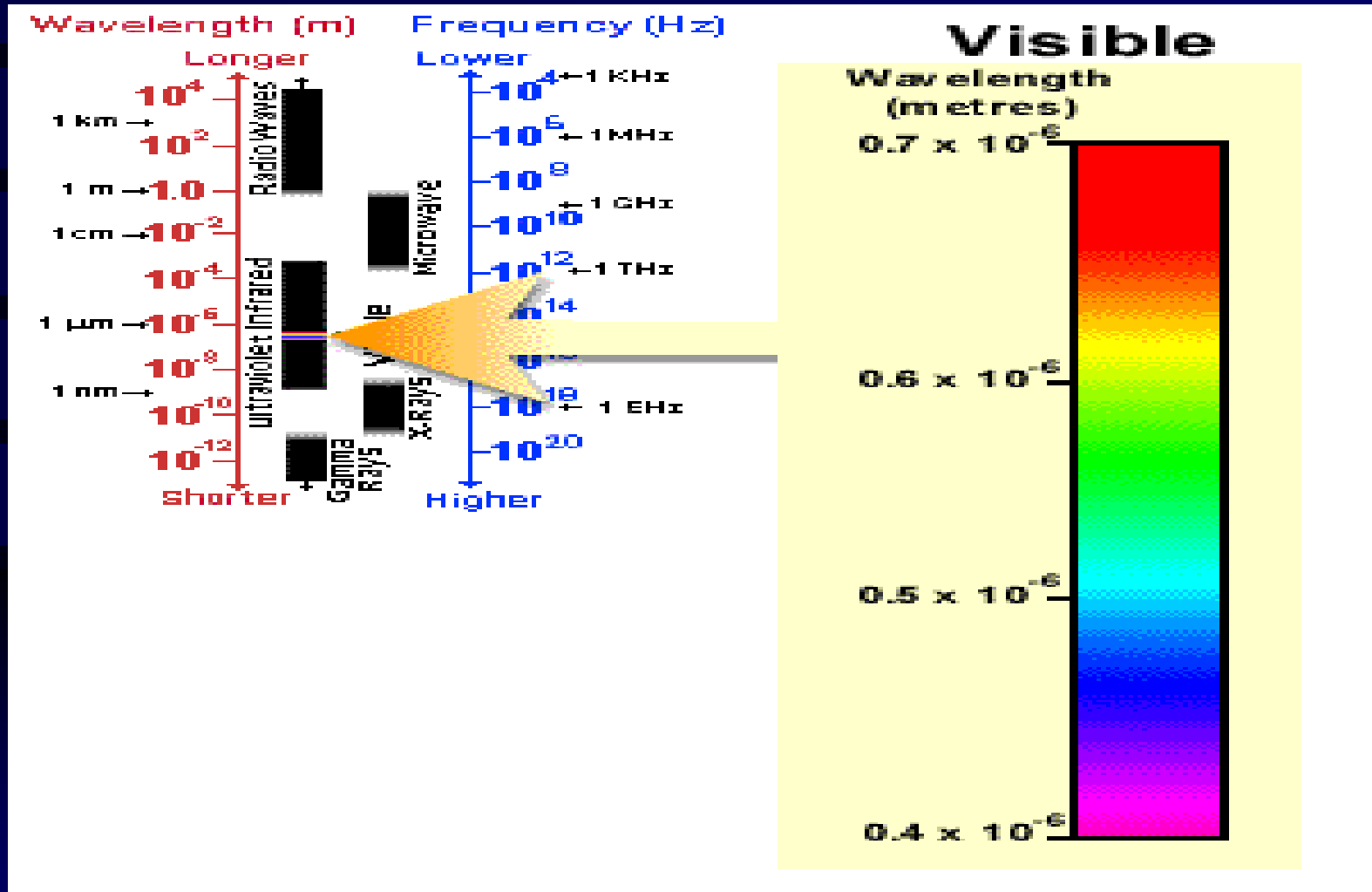


# Microwave Region of the Electromagnetic Spectrum

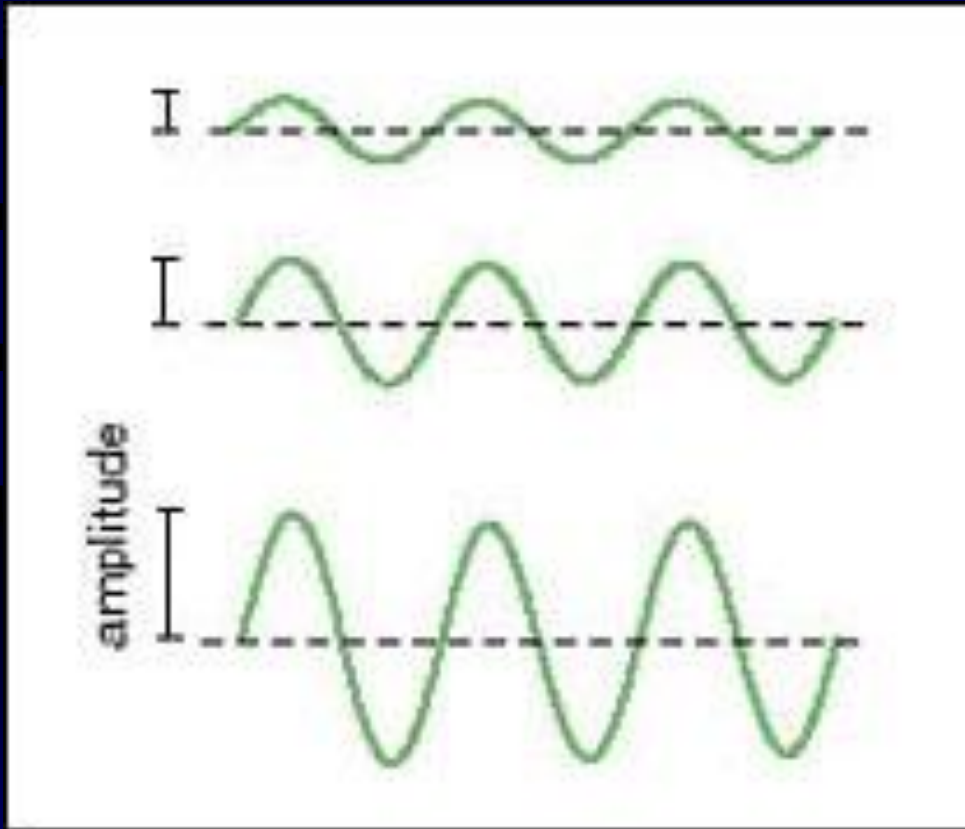




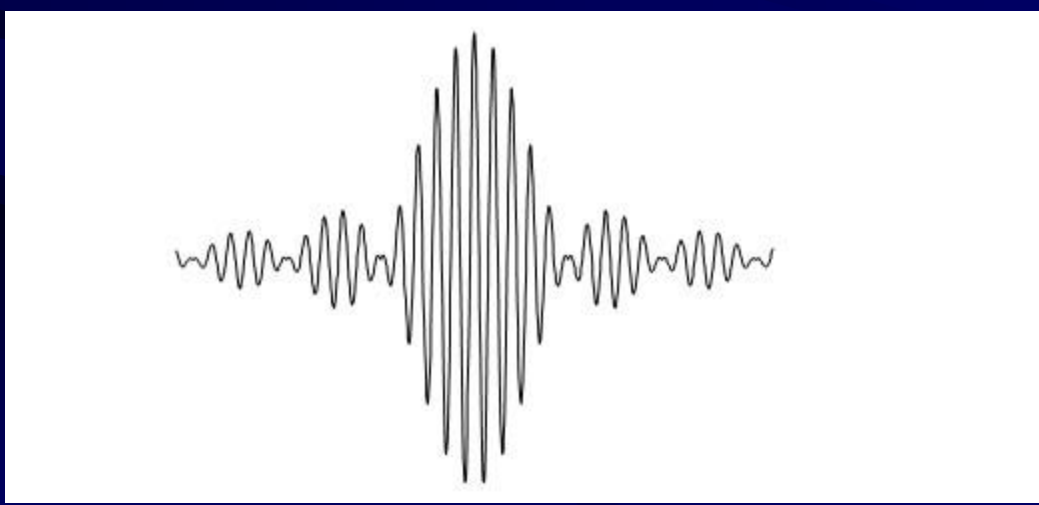
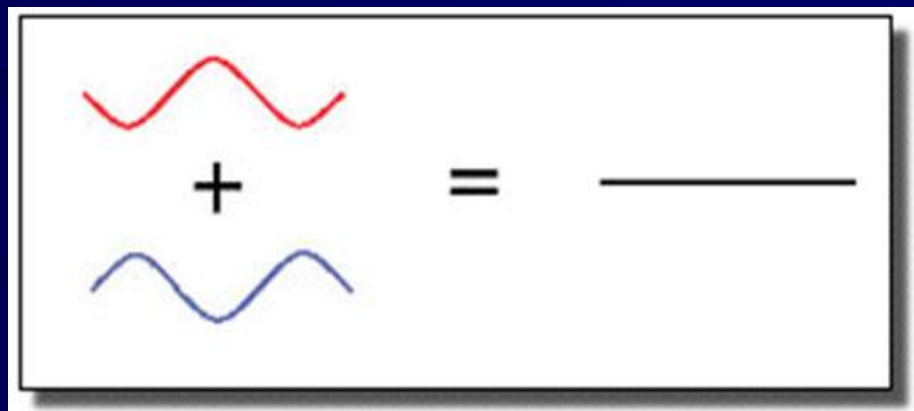
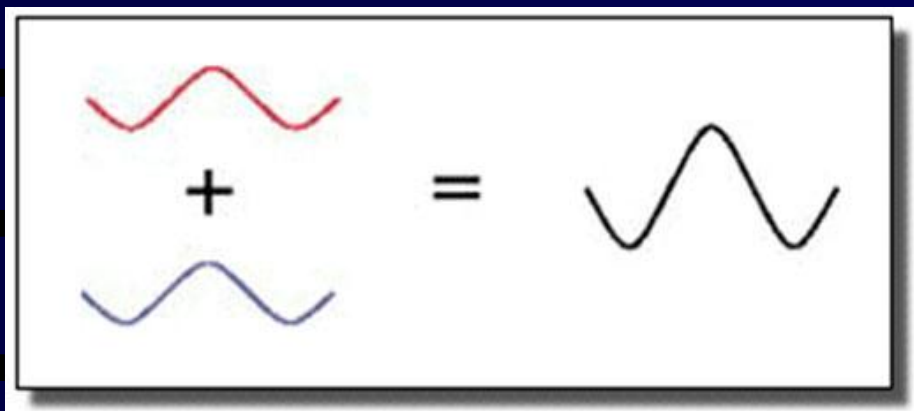
# Visible Region of the Electromagnetic Spectrum



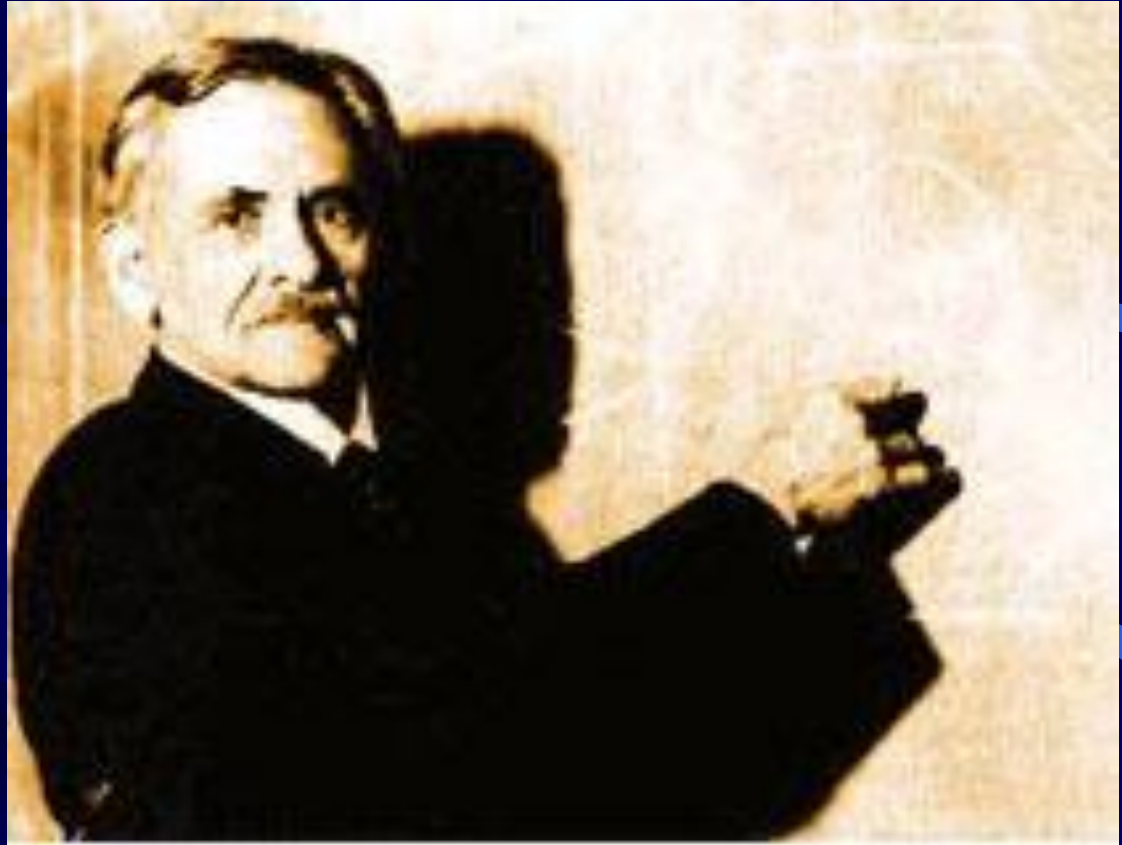
# *wave propagation*



# *wave propagation principles*



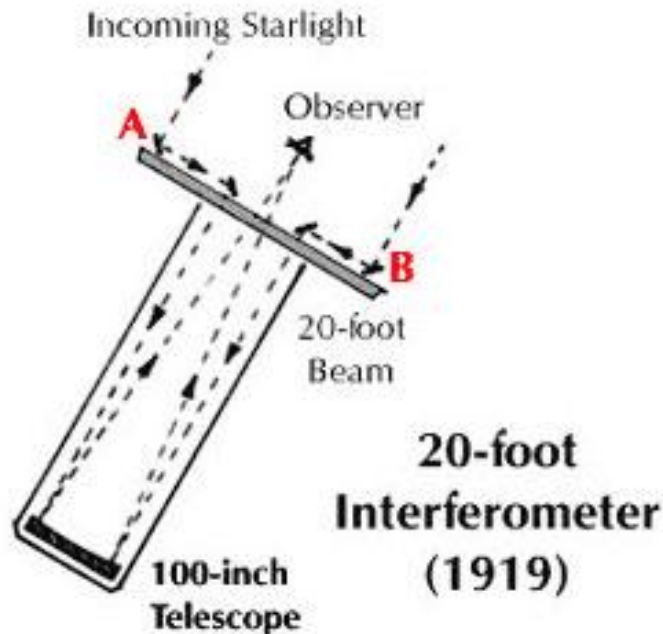
***Albert Michelson, born in 1852, Prussia  
-the pioneer of interferometry  
-in 1882 he used  
his interferometer  
to measure the  
speed of light.***



Albert Michelson

## **Primary Interferometers;**

**- in 1919 Michelson developed his 100-inch telescope to measure the diameter of remote stars.**

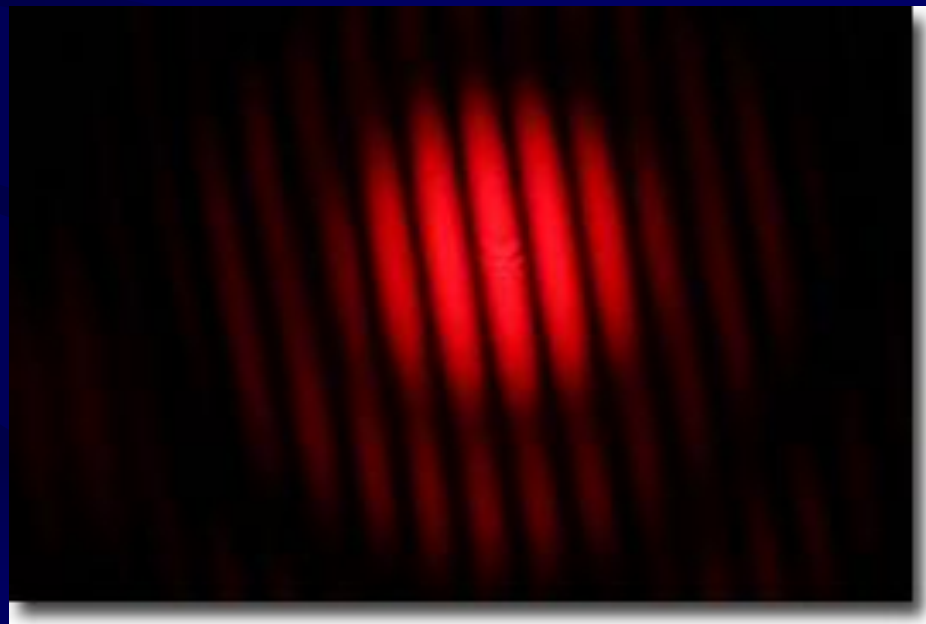
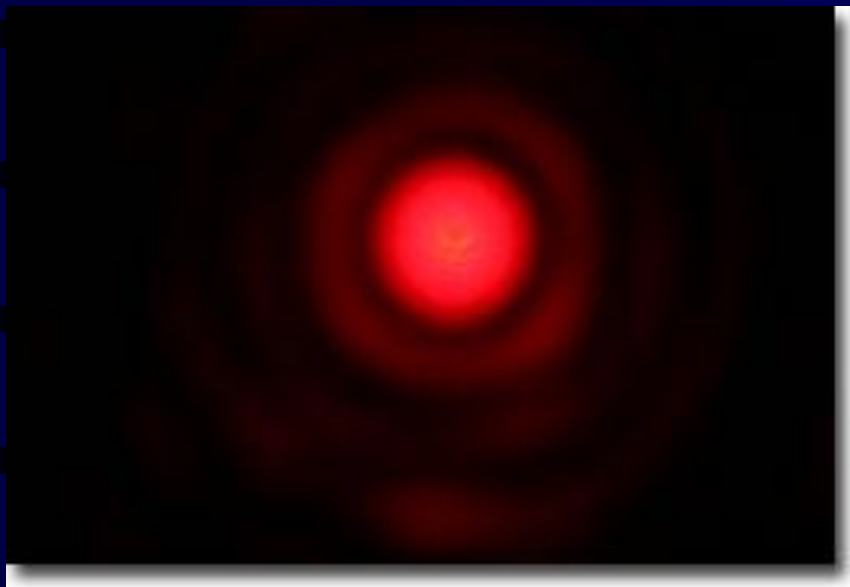


Small mirrors on the 20-foot beam directed light into the telescope. The effective diameter of the telescope has now become the distance between mirror A and B.



The 20-foot beam on top of the 100-inch Hooker Telescope on Mt. Wilson in Southern California.

## *Generating light firings by interferometry*



# **Interferometry**

<http://planetquest.jpl.nasa.gov/SIM/Demo/simford7.html>

<http://planetquest.jpl.nasa.gov/SIM/Demo/index.cfm>

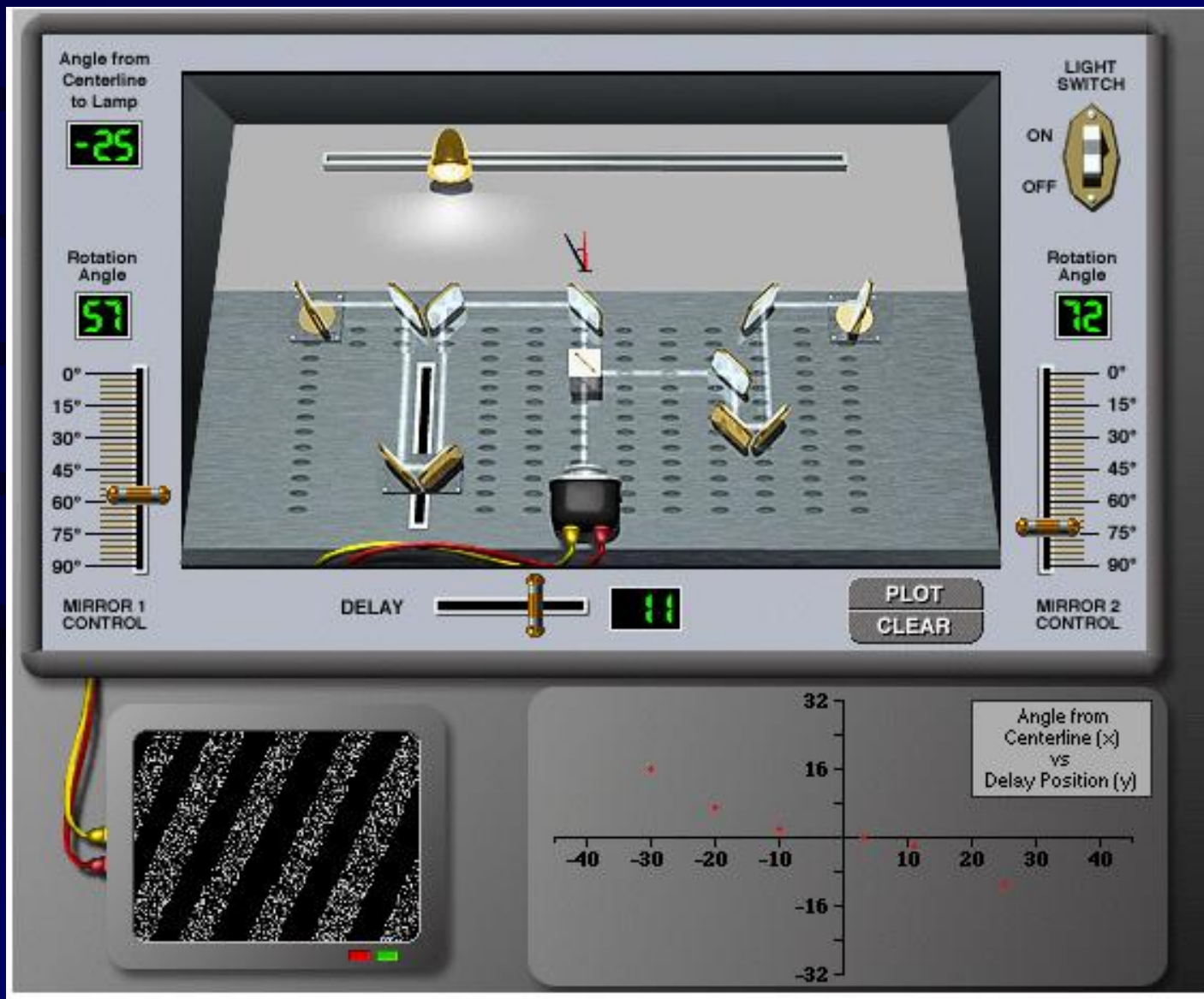
[http://planetquest.jpl.nasa.gov/SIM/sim\\_index.cfm](http://planetquest.jpl.nasa.gov/SIM/sim_index.cfm)

# Virtual Interferometer





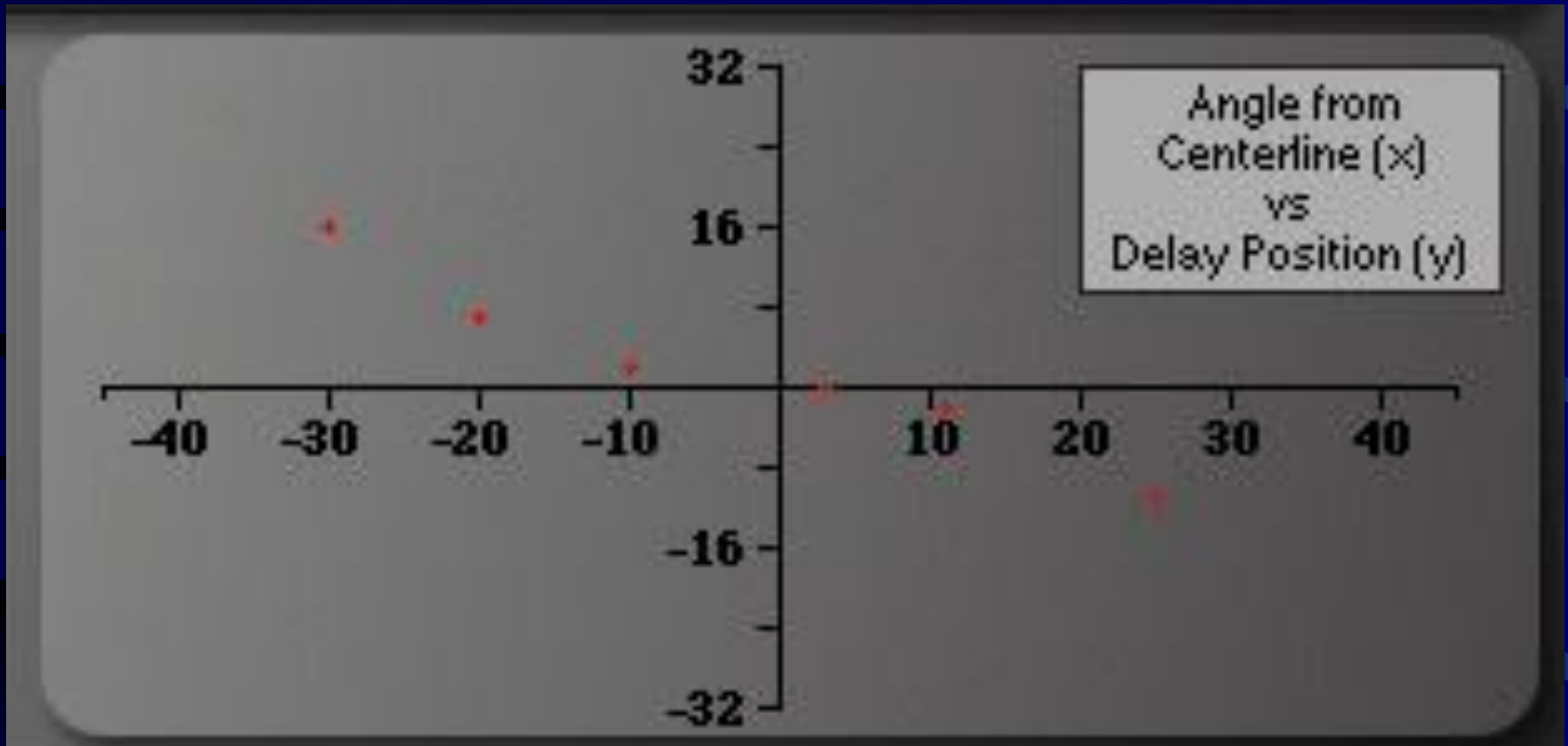
# Virtual Interferometer



The image shows a virtual control panel for an interferometer. At the top center is a 3D schematic of the optical setup, including a lamp, mirrors, and a camera. The panel features several controls and displays:

- Angle from Centerline to Lamp:** A digital display showing -25.
- Rotation Angle:** A digital display showing 57.
- MIRROR 1 CONTROL:** A vertical scale from 0° to 90° with a slider set at approximately 60°.
- MIRROR 2 CONTROL:** A vertical scale from 0° to 90° with a slider set at approximately 75°.
- LIGHT SWITCH:** A toggle switch currently in the ON position.
- DELAY:** A horizontal slider control.
- PLOT CLEAR:** Two buttons for data management.
- Angle from Centerline (x) vs Delay Position (y):** A scatter plot with axes ranging from -40 to 40 on the x-axis and -32 to 32 on the y-axis. Several red data points are plotted.
- Interferogram:** A small window showing a grayscale interference pattern with diagonal fringes.

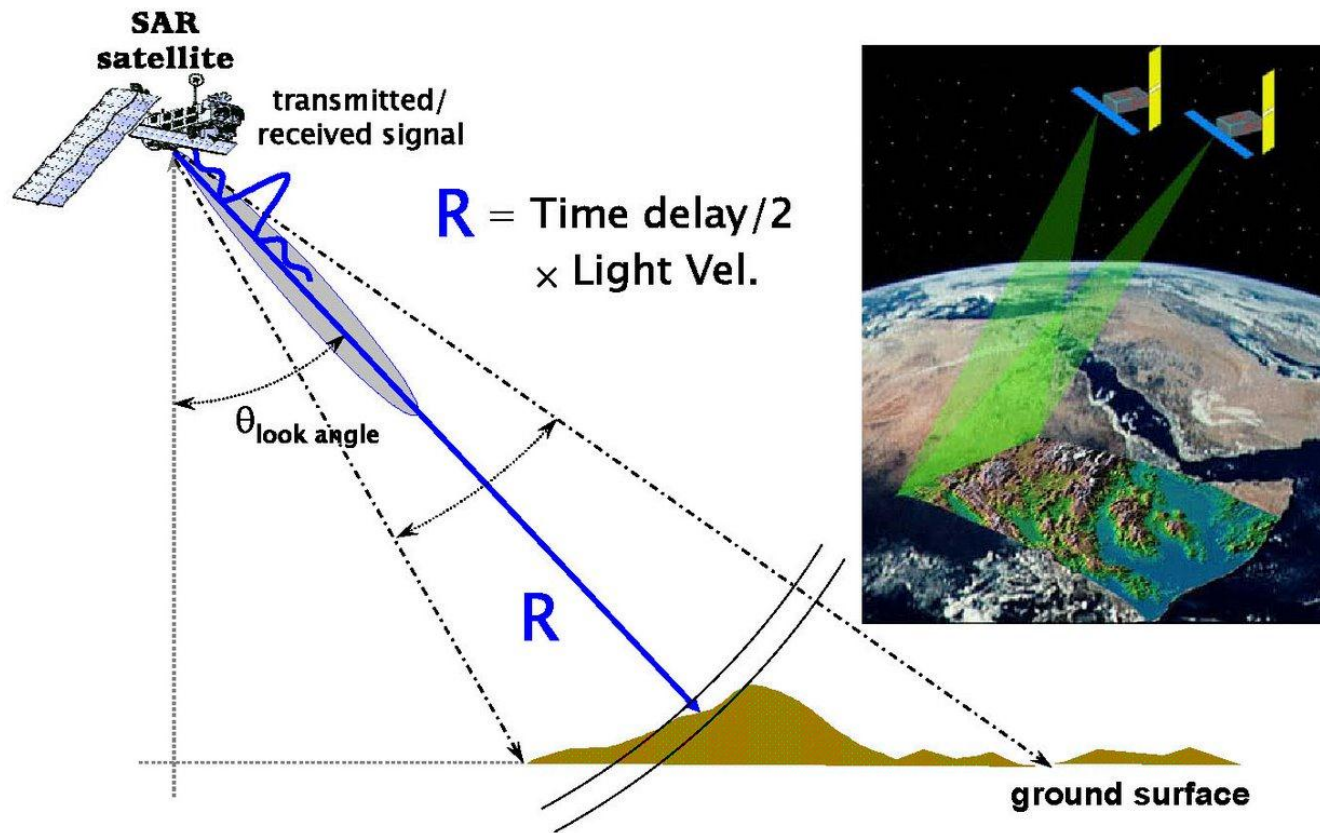
# Virtual Interferometer



*The graph of a polynomial function of degree 3*

$$y = c_0 + c_1 \cdot x + c_2 \cdot x^2 + c_3 \cdot x^3$$

# What is the origin in the real world?



# Sensor technology

## Data formats

- Raw Data
- SLC (Single Look Complex) Data
- Intensity

# Sensor technology (continued)

## Raw Data

The raw data contains the information about the object on the ground related to Azimuth Bandwidth and Range Bandwidth. Data is stored in two layers known as **real** and **imaginary** layers. These two layers contain information about all the objects in **azimuth direction** as well as in **range direction**.

# Sensor technology (continued)

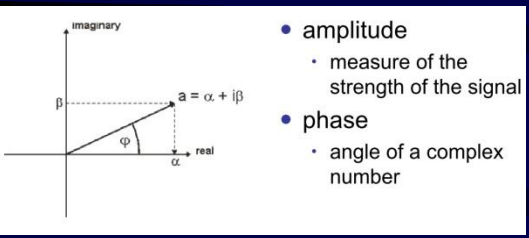
## SLC Data

SAR raw data needs to be processed before getting meaningful image.

Transformation from raw data to SLC is done by range compression and azimuth focusing.

Signal information stored in complex numbers consisting of **real** and **imaginary** component.

Using the ratio of the component, we can compute the phase and computing the length of the vector, we can derive the intensity.



## SAR SLC observations



SLC: Single-Look Complex data

- Single-look: no averaging, finest spatial resolution

- Complex: both real and imaginary (In-phase and quadrature phase) stored

$$y_1 = |y_1| \exp(j\psi_1)$$

Amplitude

Phase

*Coherent imaging*

Uninterpretable, due to scattering

$$\beta = \frac{L}{\lambda}$$

*Azimuth resolution*

# Sensor technology (continued)

## Intensity

An SLC image is transformed into an **Intensity image** by computation of the norms of the complex vectors.

### SAR SLC observations



SLC: Single-Look Complex data

- Single-look: no averaging, finest spatial resolution

- Complex: both real and imaginary (In-phase and quadrature phase) stored

*Coherent imaging*

$$y_1 = |y_1| \exp(j\psi_1)$$

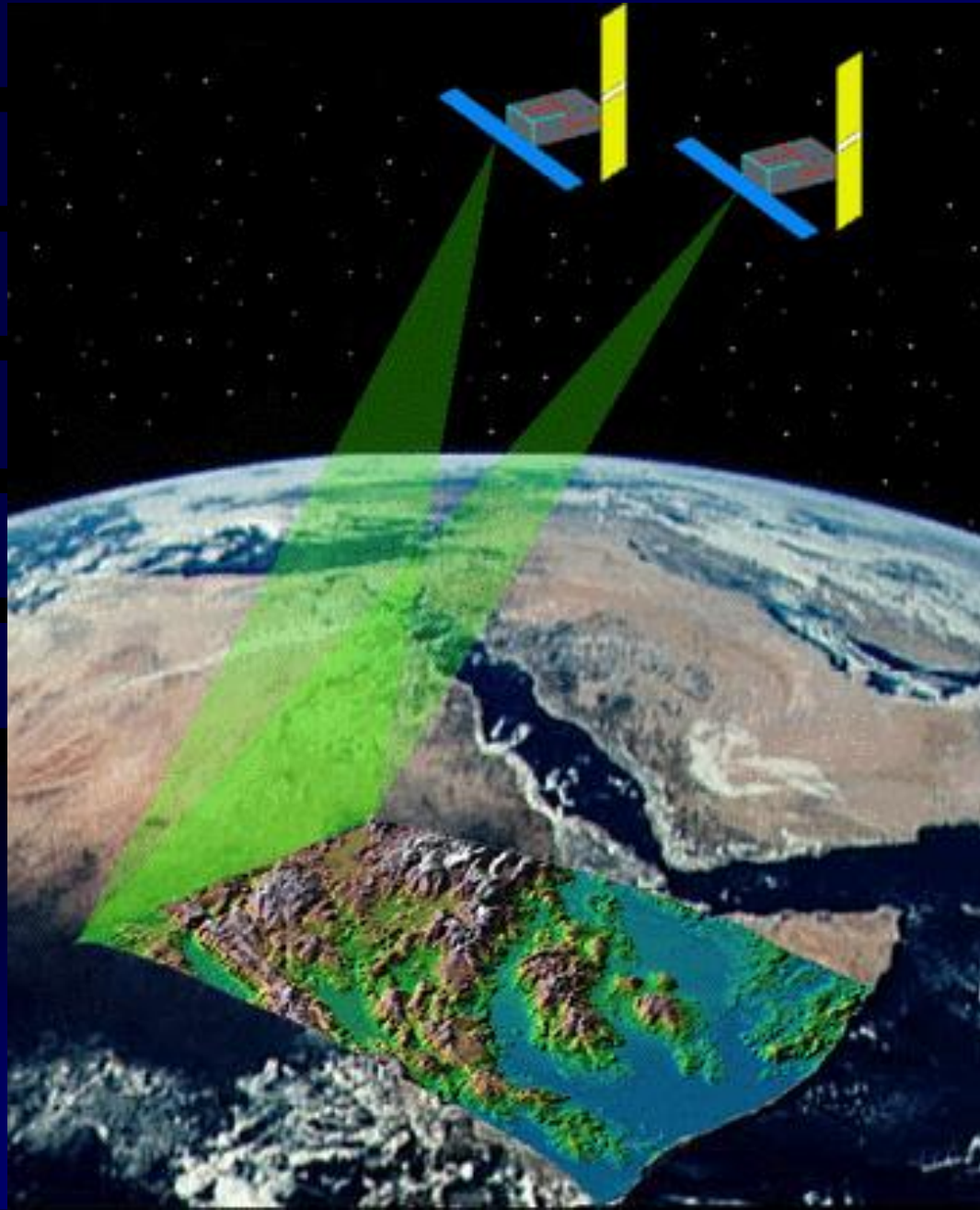
← Amplitude

Phase

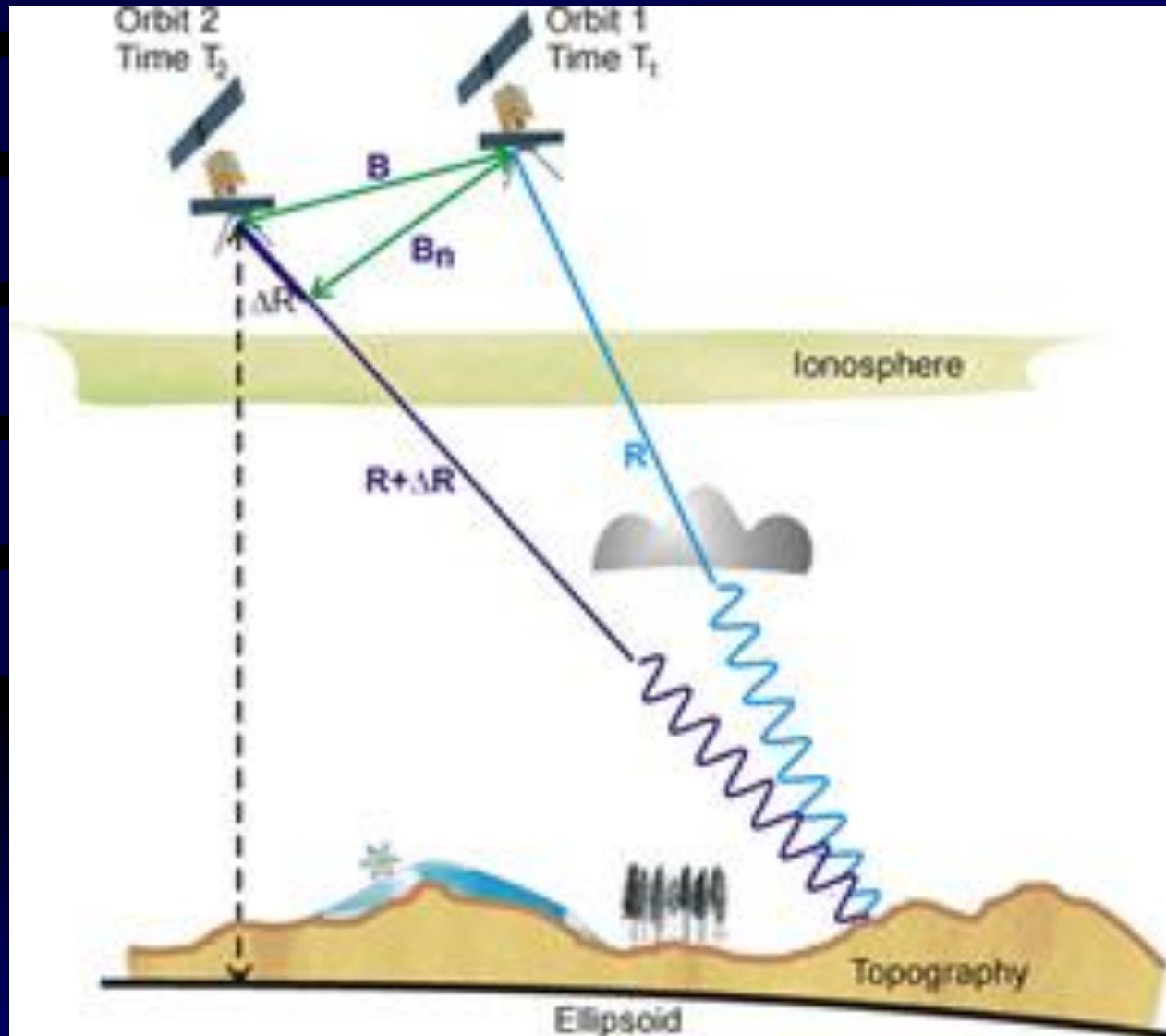
Uninterpretable, due to scattering

**Synthetic Aperture Radar  
Interferometry (InSAR)  
Technique**



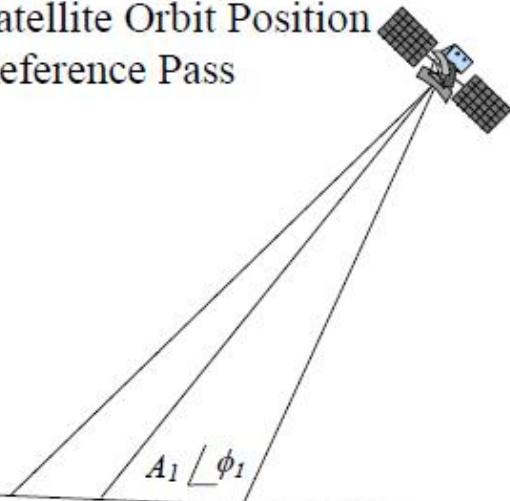


- SAR interferometry in recent years proves to be a strong method for change detection, DEM generation, classification and...
- For interferometry, two radar images of the same area with **slightly different imaging angles** is required.



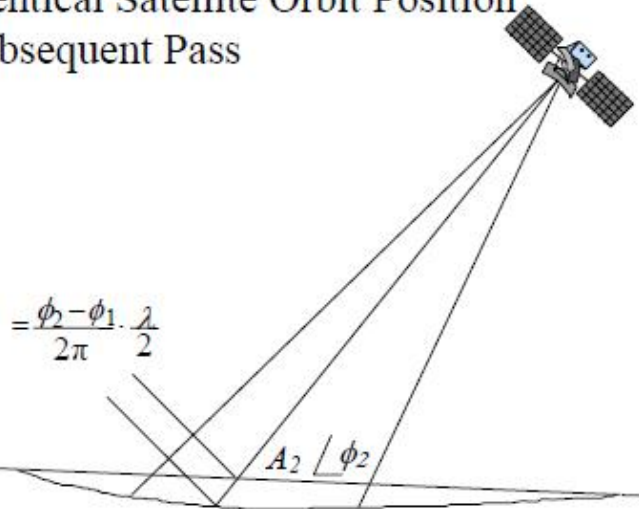
**Synthetic Aperture Radar (SAR) technology is an efficient tool for monitoring and inspection of dynamic phenomena on Earth.**

Satellite Orbit Position  
Reference Pass

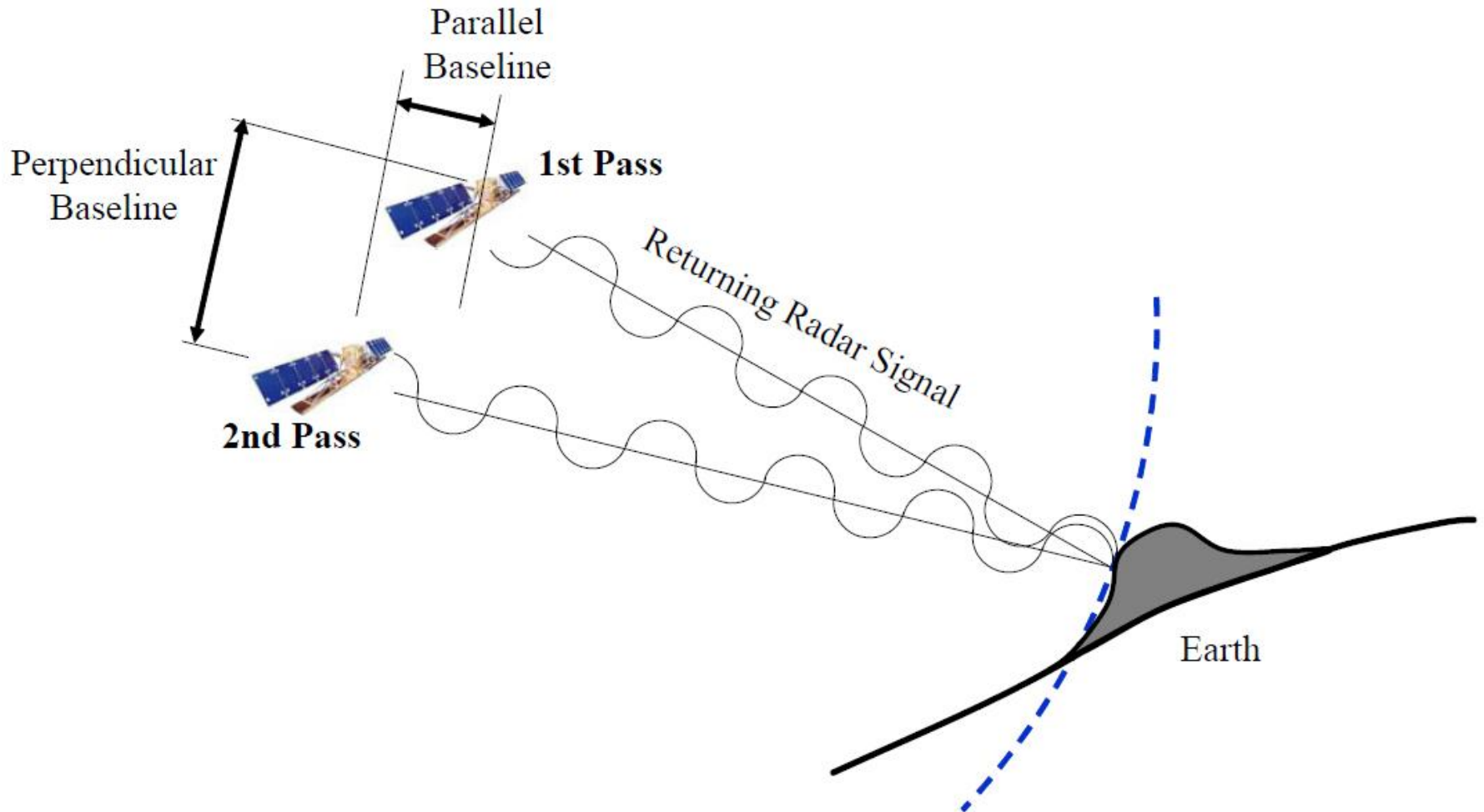


Identical Satellite Orbit Position  
Subsequent Pass

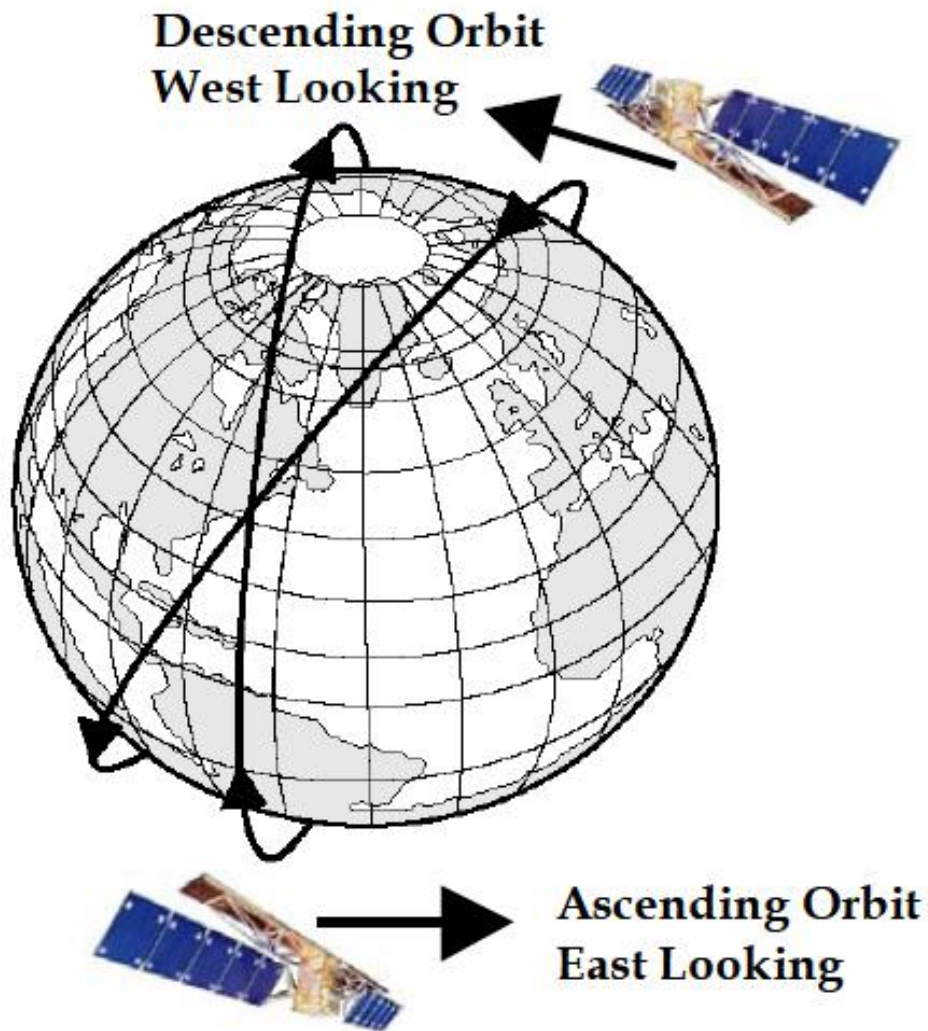
$$d = \frac{\phi_2 - \phi_1}{2\pi} \cdot \frac{\lambda}{2}$$



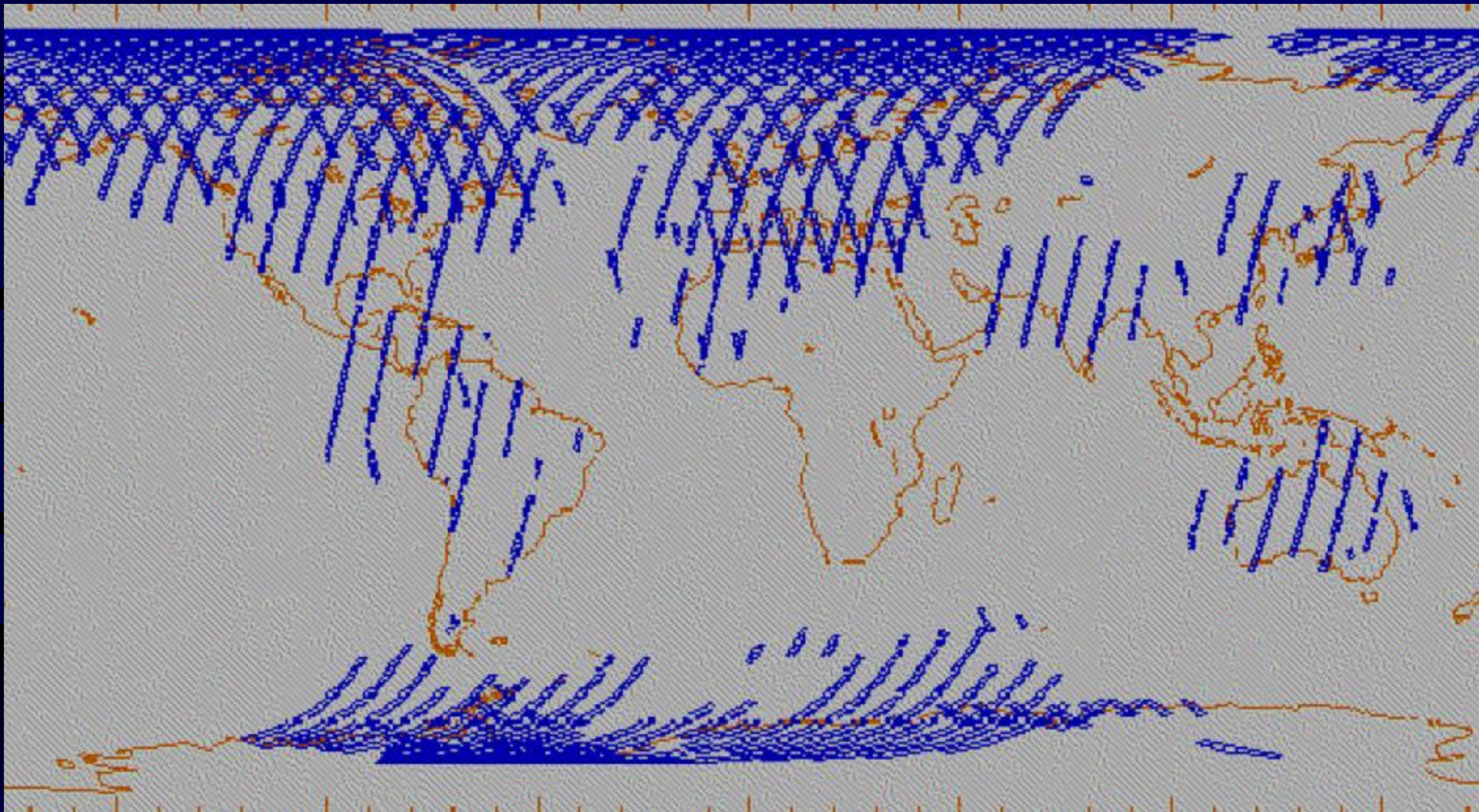
**InSAR measurement of ground movement**



**Orbit baseline changes can produce varying phase shifts.**

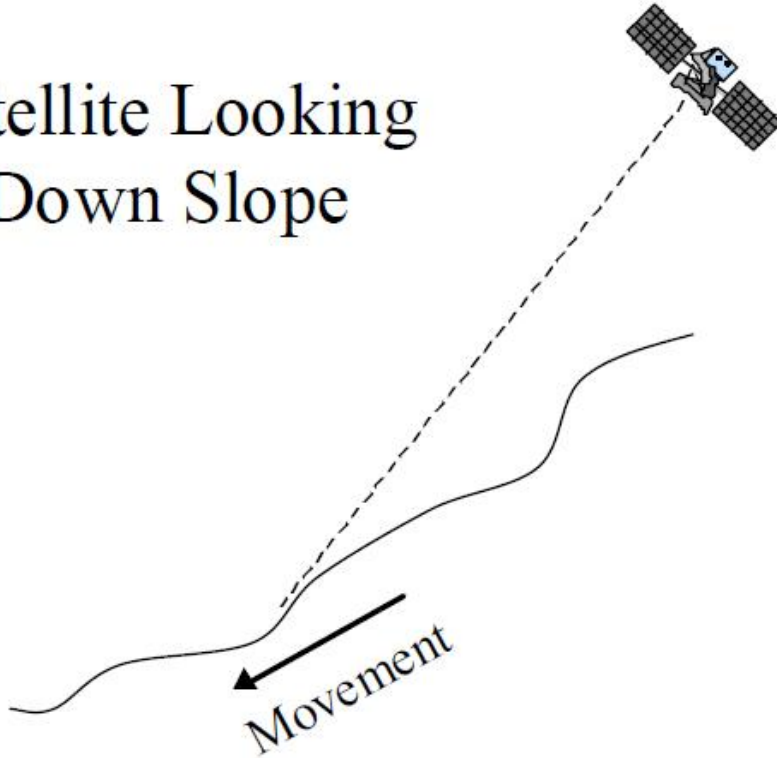


**Polar orbiting satellites have an east looking and west looking perspective.**

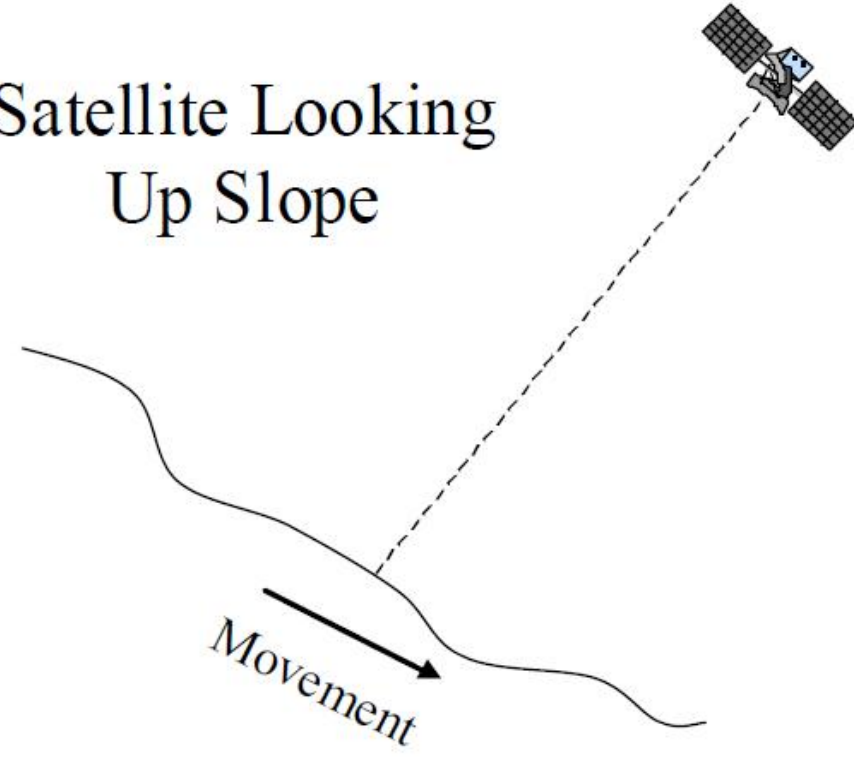


**ERS 1 & 2 tracks  
800 km height, ascending/descending near polar orbit,  
35 days repeat period**

Satellite Looking  
Down Slope



Satellite Looking  
Up Slope



**Example of satellite looking up-slope and  
down-slope**

## InSAR is a set of successive steps to produce a height image called DTM.

- To generate DTM's, deformation maps or thematic maps, *two or more SAR datasets of the same area acquired by the same sensor systems are needed.*

*datasets are in such a format that they still contain the phase and magnitude information of the radar signal and also the orbit, timing, calibration and other essential parameters of these data are available*

- To produce a DTM

*The following basic steps should be carried out successively*

**Data search, selection and pre-processing**

**Co-registration of the data sets**

**Coherence map generation**

**Interferogram generation**

**Phase unwrapping**

**DTM generation**



## DEM generation steps

data processing stage comprises of five steps

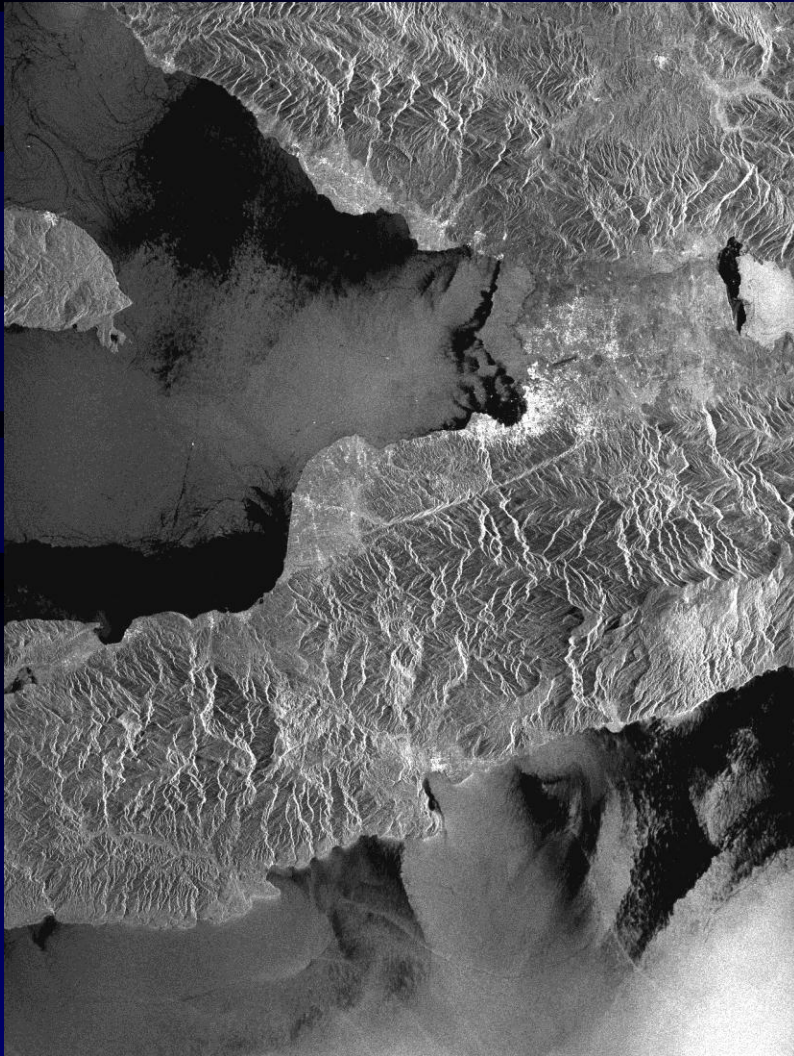
- data pre-processing
- coregistration
- interferogram generation
- phase unwrapping
- geo-coding

# Data search, selection and pre-processing

PORT-AU-PRINCE/ Jan 12, 2010: A huge quake measuring 7.0 hits Haiti.

Baseline: 279.98m

**Master image dated 26 January 2010**



**Slave image dated 2 March 2010**



## Coregistration of the data sets

**By the conventional image  
coregistration methods**

# Coherence map generation

- Optics equivalent to correlation:

$$\gamma = \frac{E\{y_1 y_2^*\}}{\sqrt{E\{|y_1|^2\} \cdot E\{|y_2|^2\}}}$$

- Estimation of coherence:

$$|\hat{\gamma}| = \frac{|\sum_{n=1}^N y_1^{(n)} y_2^{(n)}|}{\sqrt{\sum_{n=1}^N |y_1^{(n)}|^2 \sum_{n=1}^N |y_2^{(n)}|^2}}$$

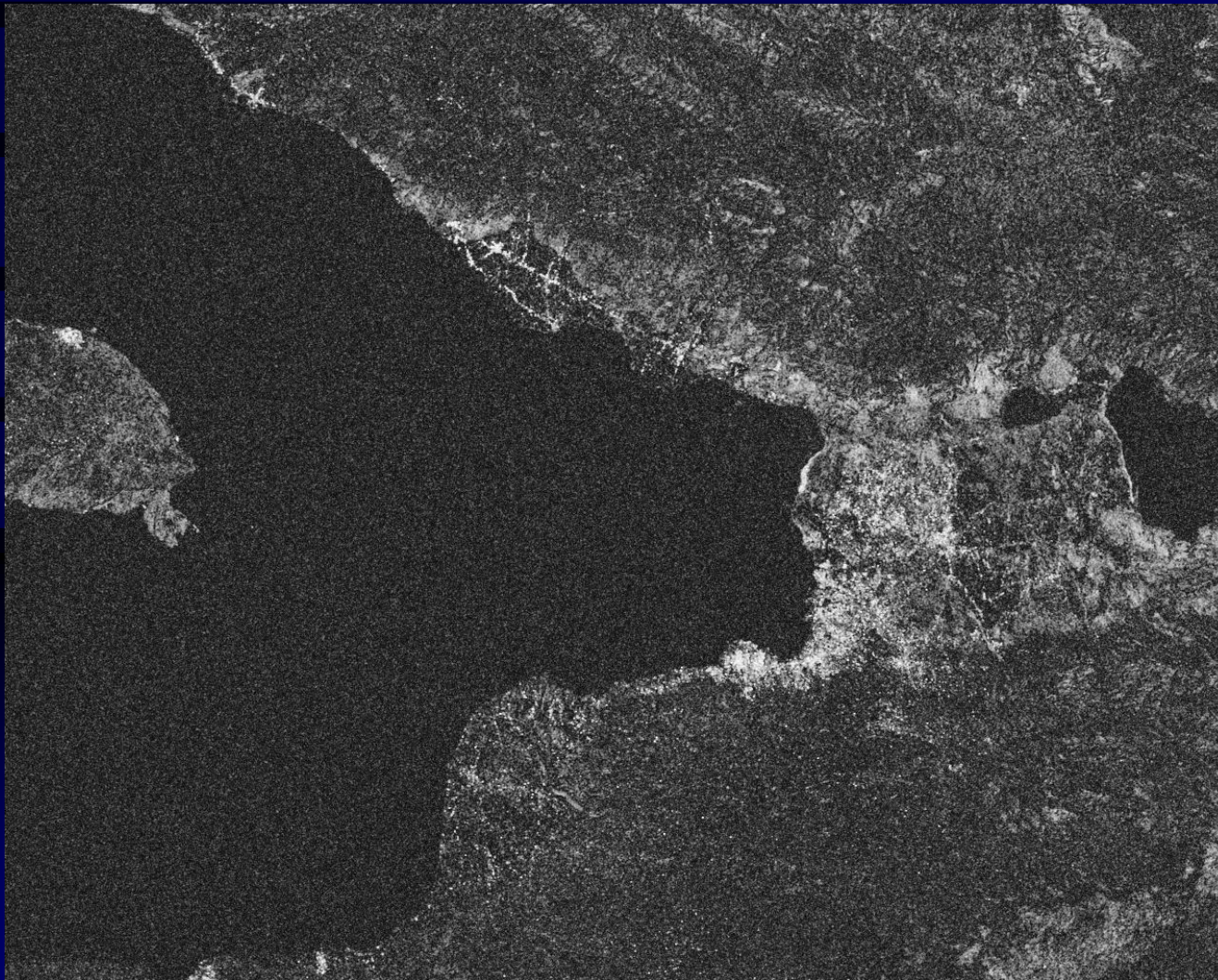
# Coherence map generation

$$\gamma = \frac{\sum_{NL}(y_1 \cdot y_2^*)}{\sqrt{\sum_{NL}(|y_1|^2) \cdot \sum_{NL}(|y_2^*|^2)}}$$

- The sums are over **L=5** looks in frequency and N spatially adjacent pixels.
- Generally large values of N will give poor spatial resolution but will help to reduce the zero coherence bias and the speckle noise.
- A value of **N=3 × 3** is the compromise, which gives a zero coherence bias of approximately **0.21**.
- Values of N greater than 1 also introduce a negative bias for high phase slopes.
- This leads to an under-estimate of the coherence in regions of high slope.
- The **coherence** is always a non-negative real number limited between **0** (for totally different images) and **1** (for completely identical images).
- Due to the moving window transient, the coherence image shows a border which size is half the moving window size, consisting of null pixels.

# Coherence map generation

Coherence image of the data pairs of  
master image dated 26 January 2010 and slave image dated 2 March 2010



Measure for the  
correlation of  
corresponding  
signals

Ranges from  
0 to 1

# Interferogram generation

$$I(m, n) = A_1(m, n) A_2^* (m, n) e^{i\Phi(m, n)}$$

The complex pixel  $(m, n)$  of a SAR image can be written as an amplitude  $A$  and phase term  $\Phi$ .

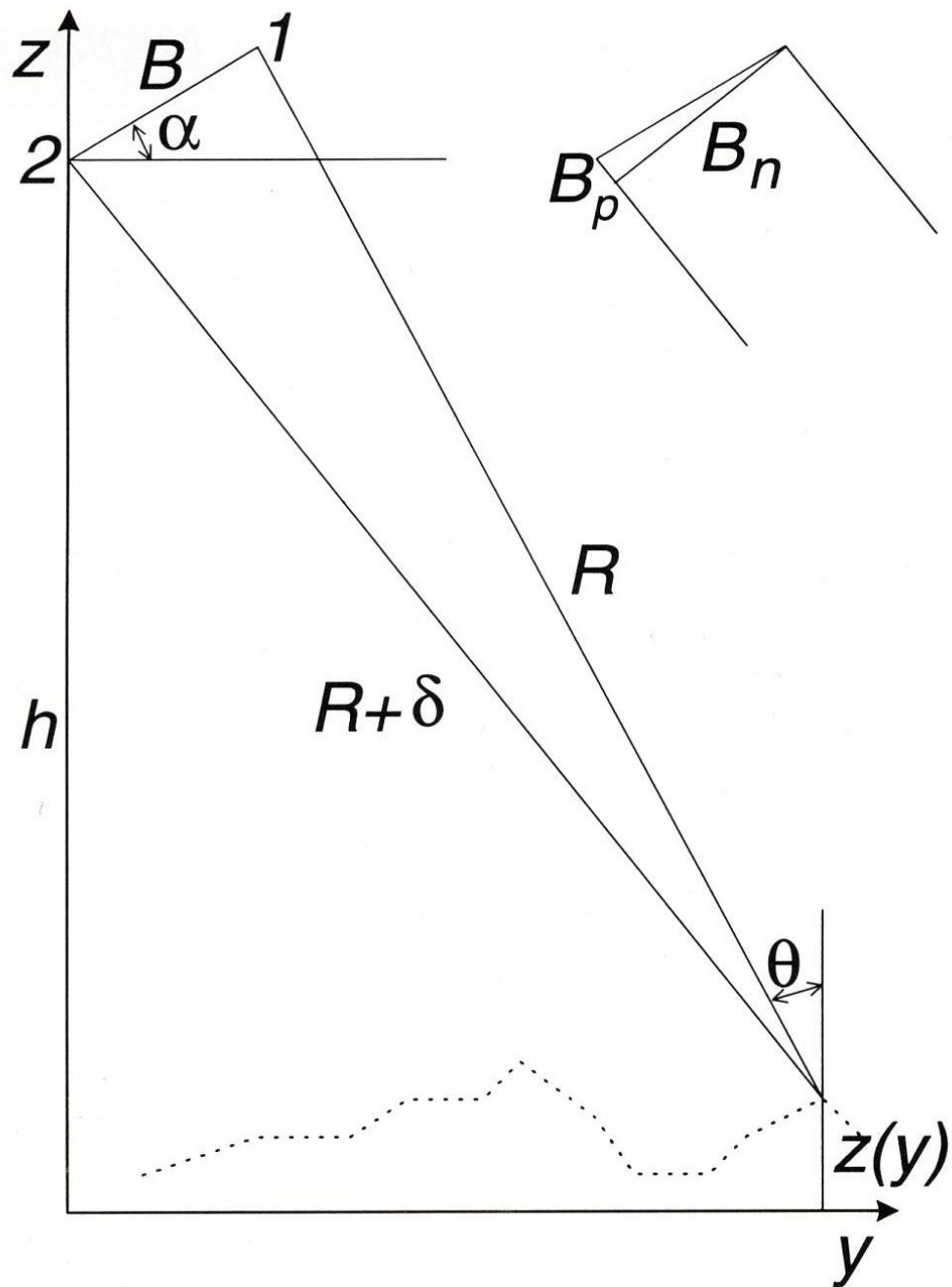
The phase term in above equation represents the difference in phase shift caused by the two-way propagation of the radar signal to the ground.

$$d\Phi = \frac{4\pi B_n}{\lambda R \sin \theta} [dz + \cos \theta dR] = d\phi_z + d\phi_R$$

$B_n$  normal baseline,  $\lambda$  radar wavelength,  $R$  range and  $dR$  change in range,  $dz$  change in surface height,  $\theta$  the local incidence angle

$$dz = \frac{\lambda R \sin \theta}{2B_n}$$

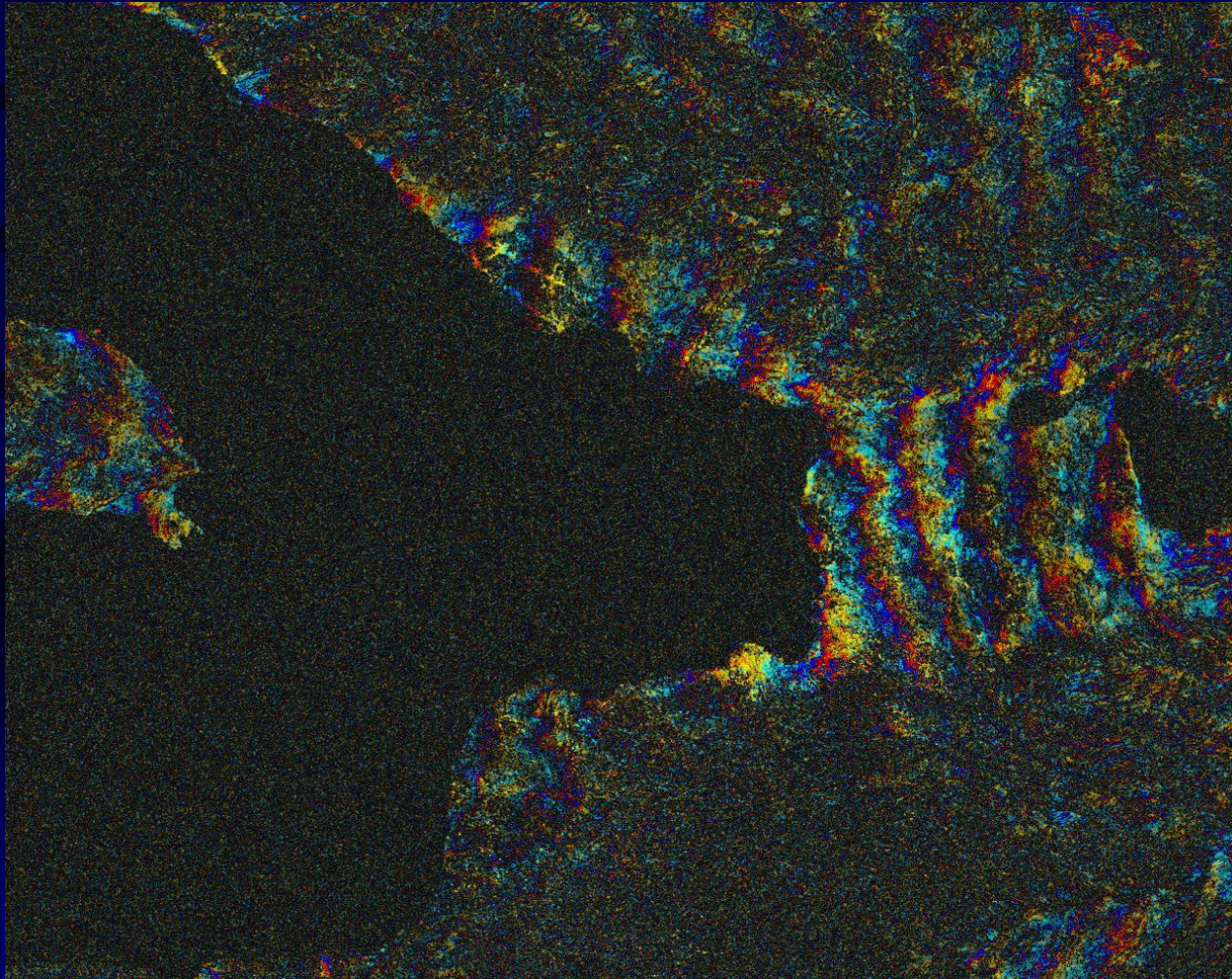
InSAR Geometry





# Interferogram generation

Interferogram of the data pairs of  
master image dated 26 January 2010 and slave image dated 2 March 2010

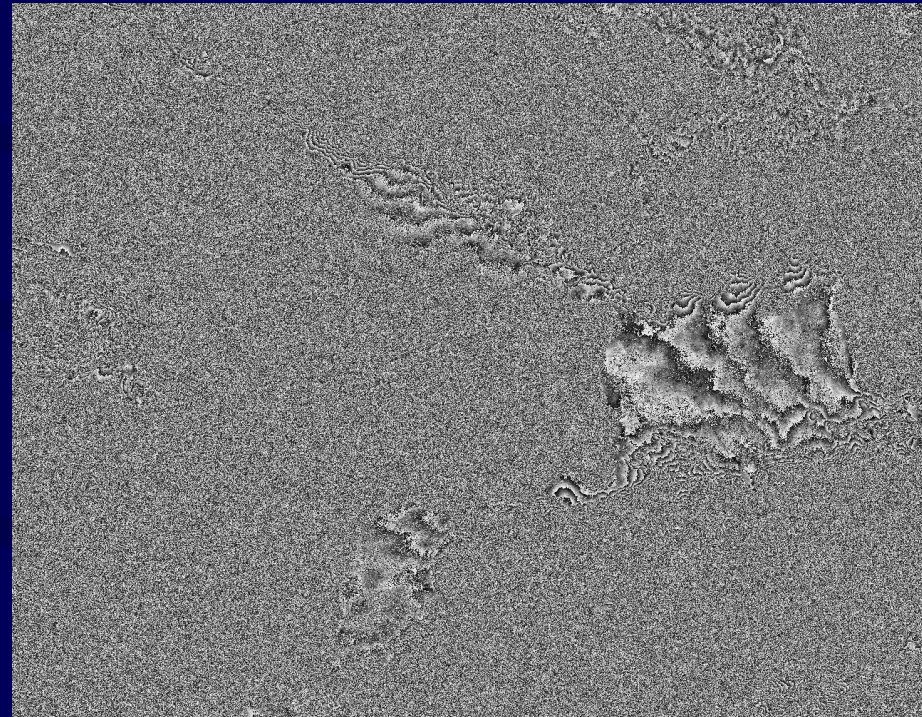
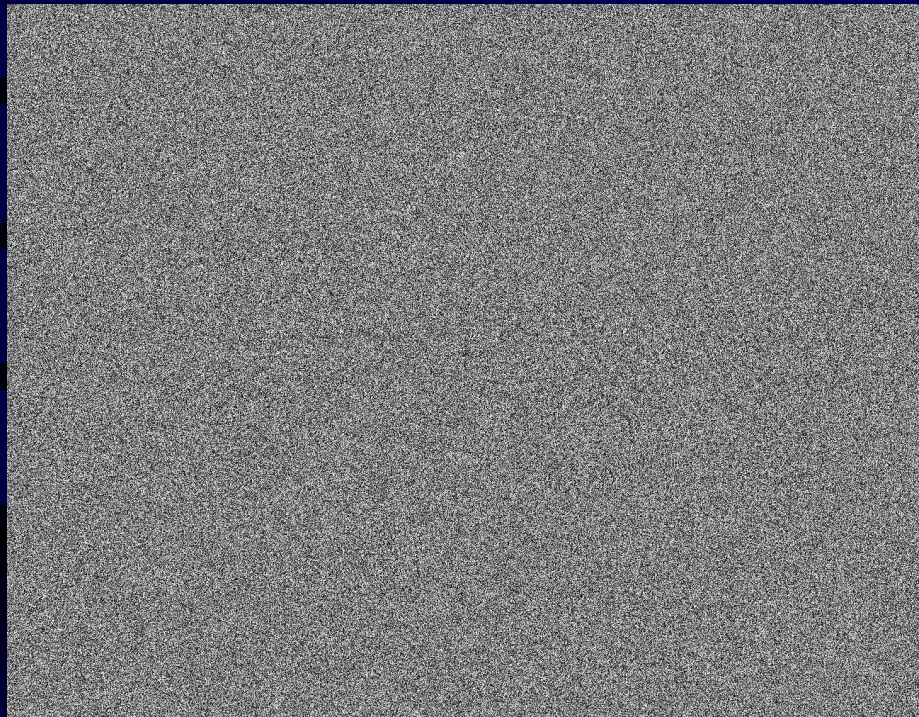


# Phase unwrapping

Phase image and unwrapped phase of the data pairs of  
master image dated 26 January 2010 and slave image dated 2 March 2010

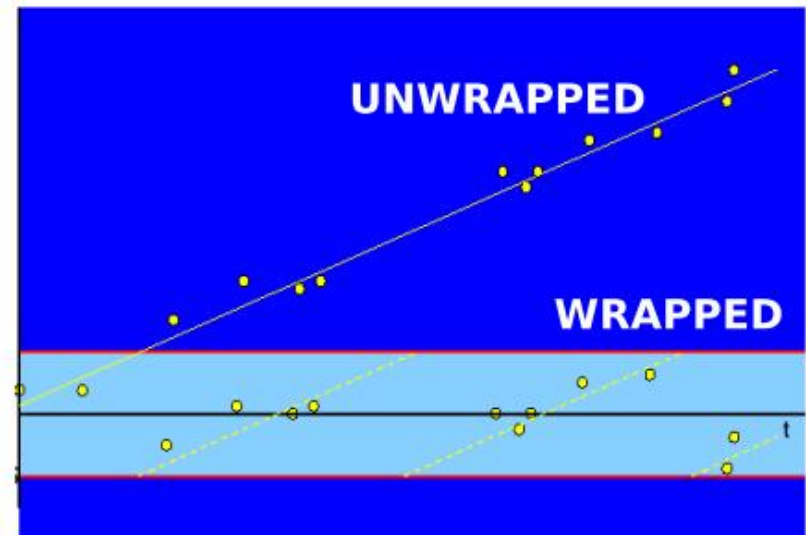
Phase image

unwrapped phase image



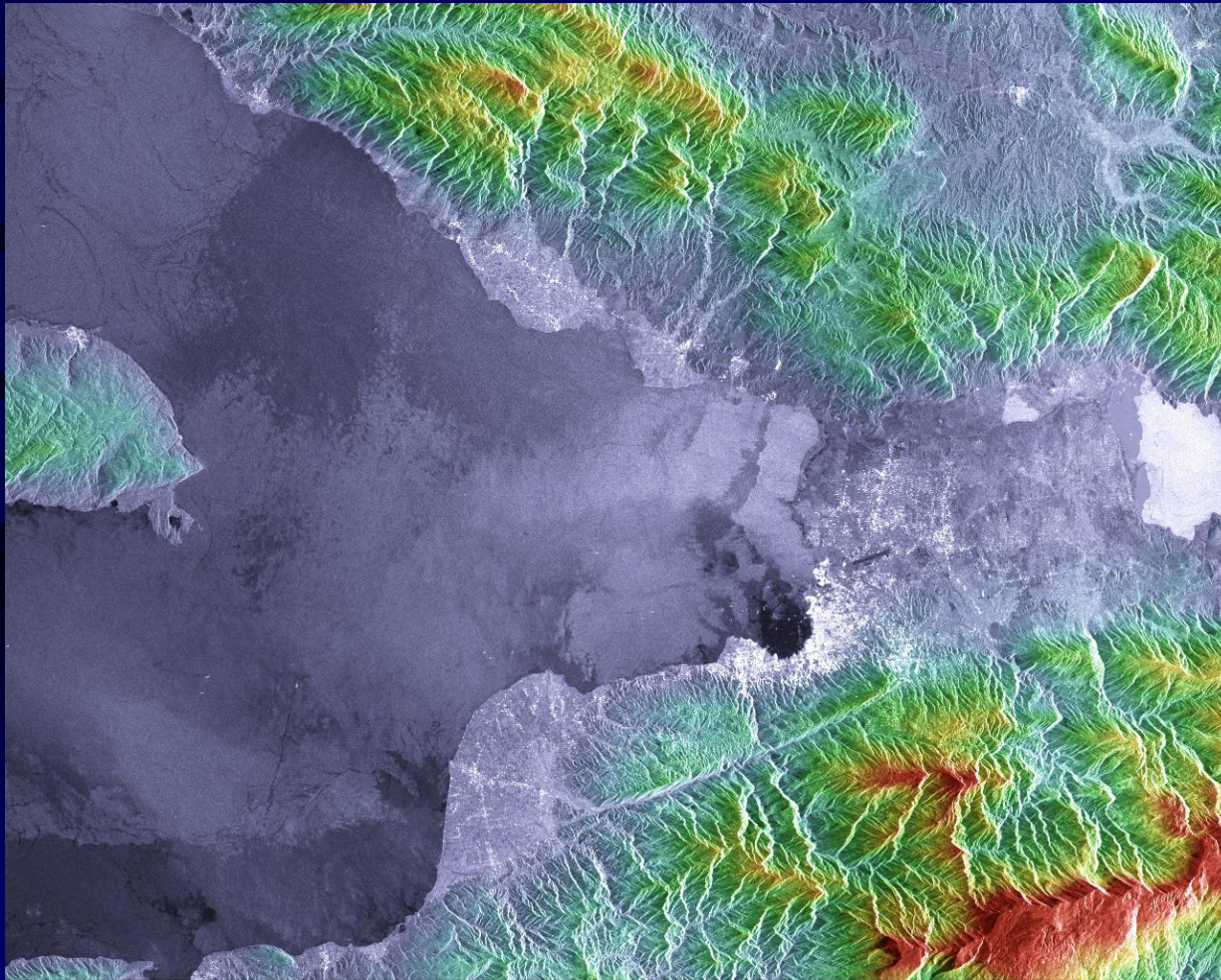
## Interferometric phase notion: a simplified example

- The observed phase is wrapped in  $[-\pi, +\pi]$
- Interpretation requires the absolute phase
- Simplified example:
  - a point is moving away from the radar with constant velocity,
  - phase unwrapping is the most complicated processing step.
  - hampered by decorrelation and dense fringes

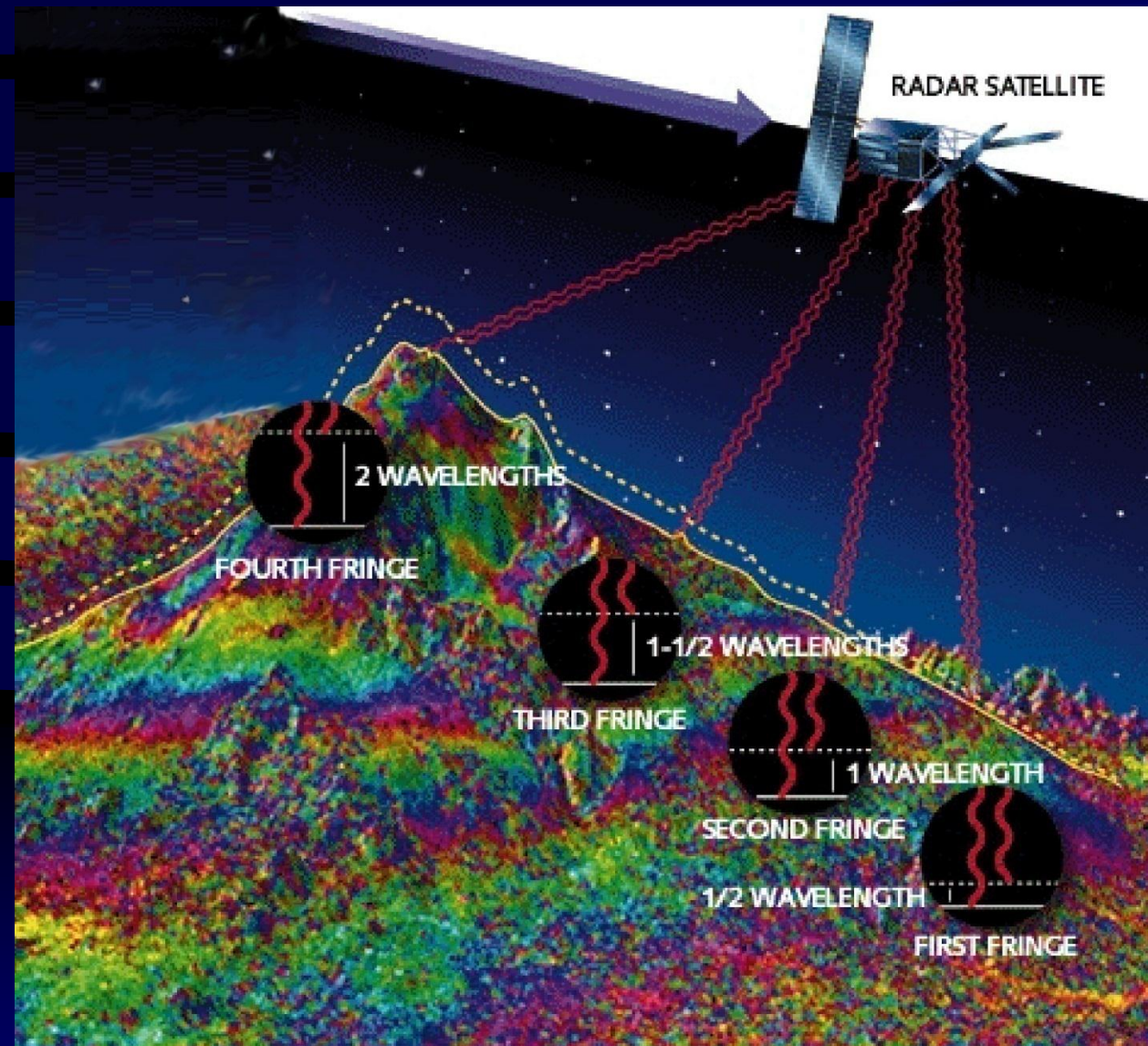


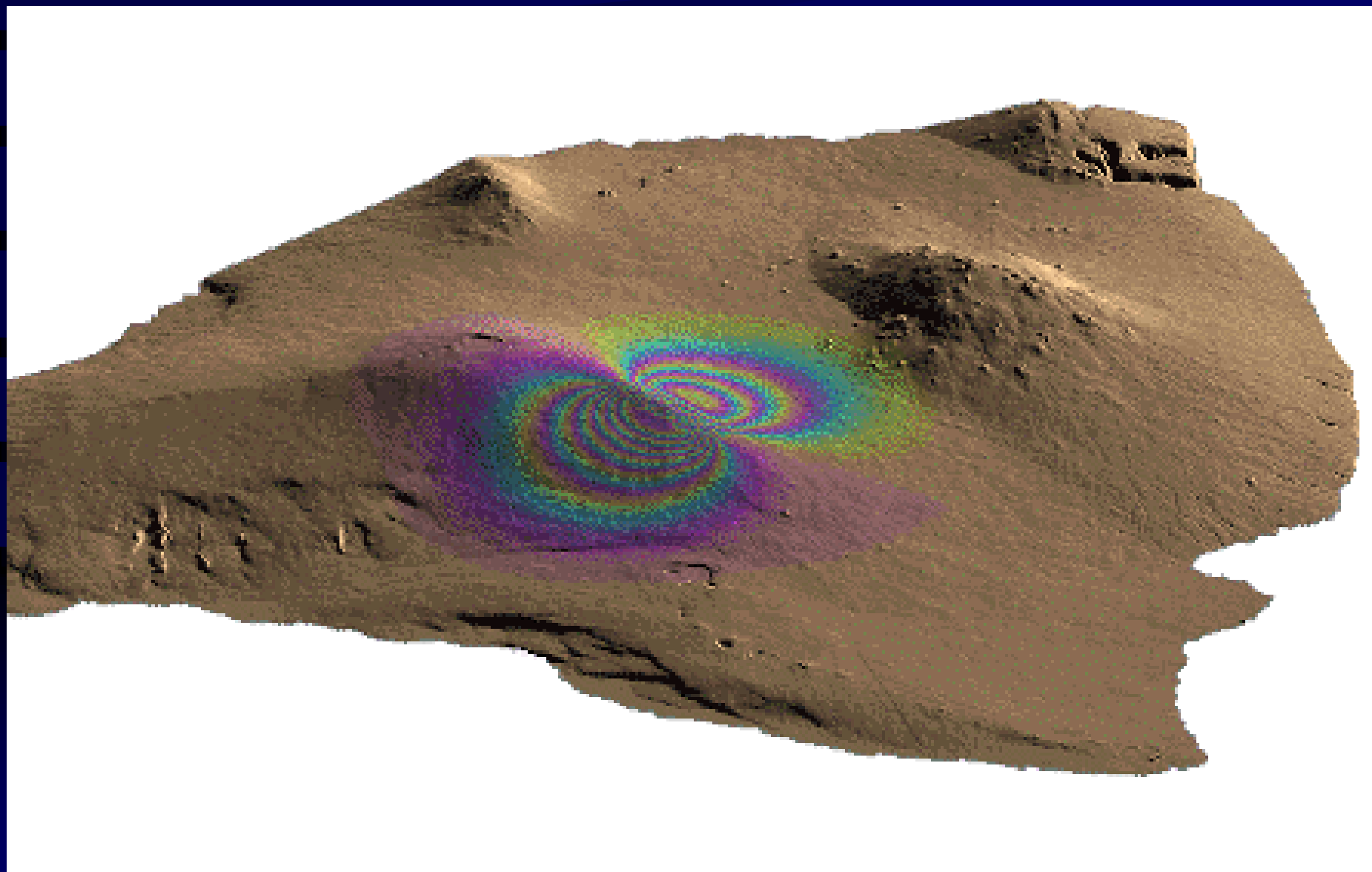
# DTM generation

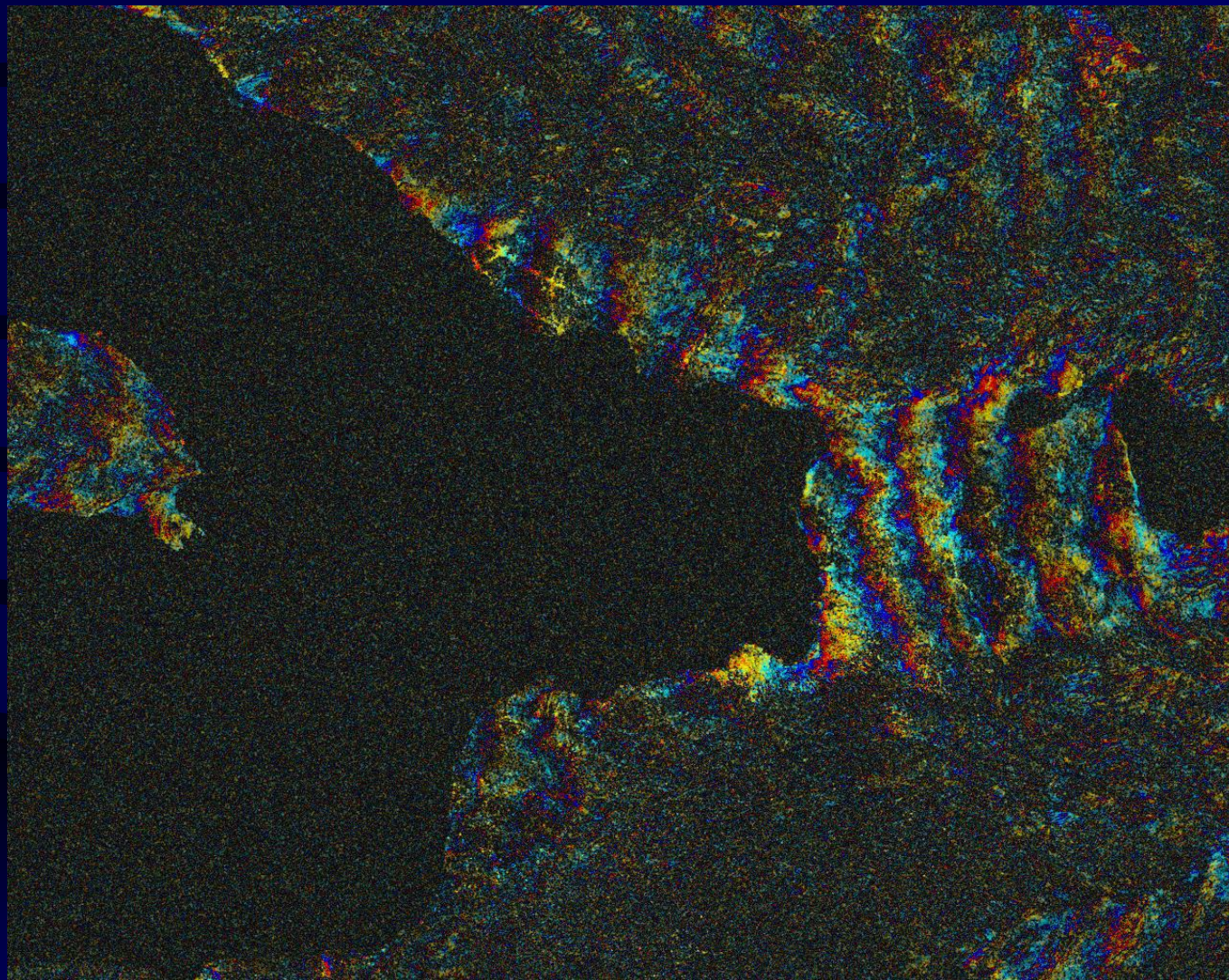
Topo-map of the data pairs of  
master image dated 26 January 2010 and slave image dated 2 March 2010



An interference model





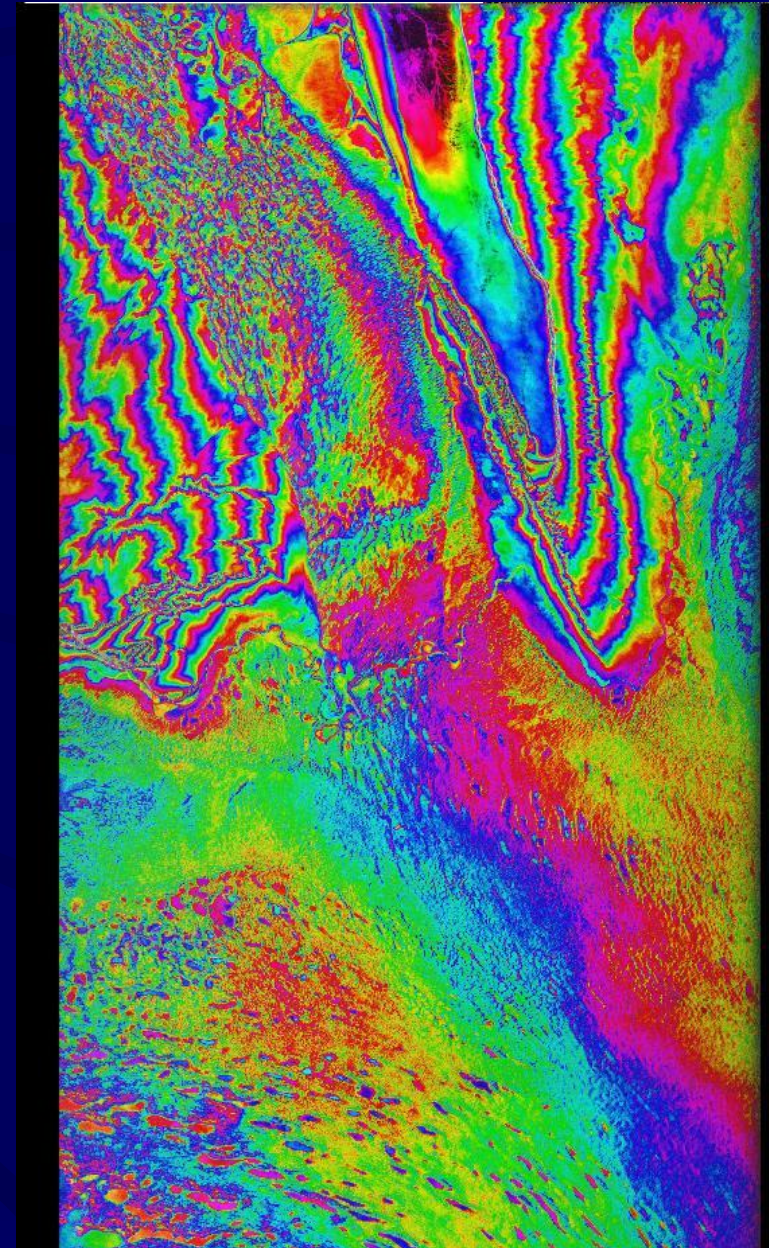


**Interferogram of the data pairs of  
master image dated 26 January 2010 and slave image dated 2 March 2010  
PORT-AU-PRINCE, Haiti** **Baseline: 279.98m**

## ***Interferogram:***

- can be generated by complex computerized processes from phase data of two radar imagery of a common area of the Earth surface collected in two different times.
- consists of the fringes cycling from yellow to purple to turquoise and back to yellow.
- Representing the whole range of the phase from 0 to  $2\pi$  in a full color cycle

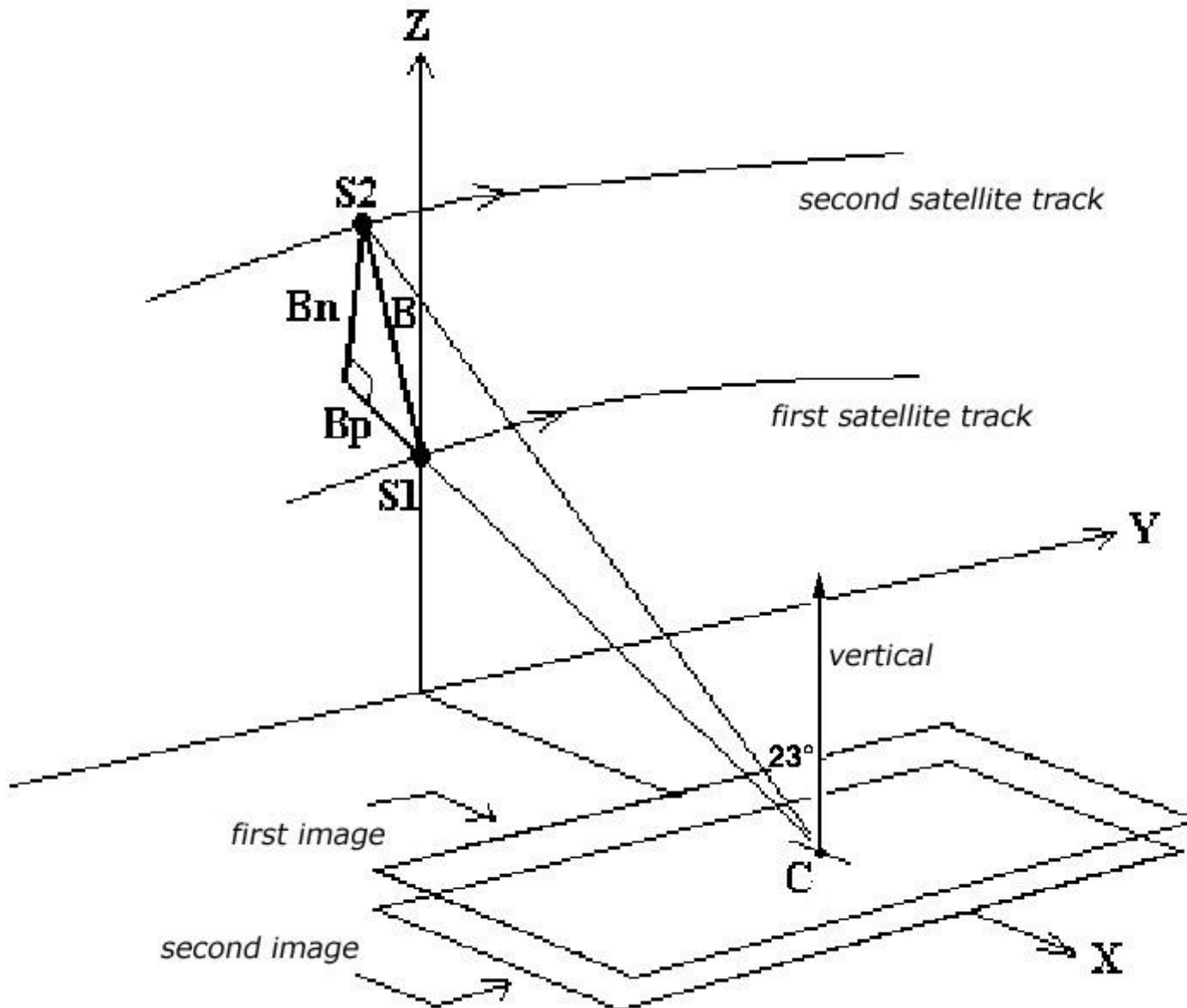
*Each cycle represents a change in the ground height in the direction of platform that depends on satellite geometry.*



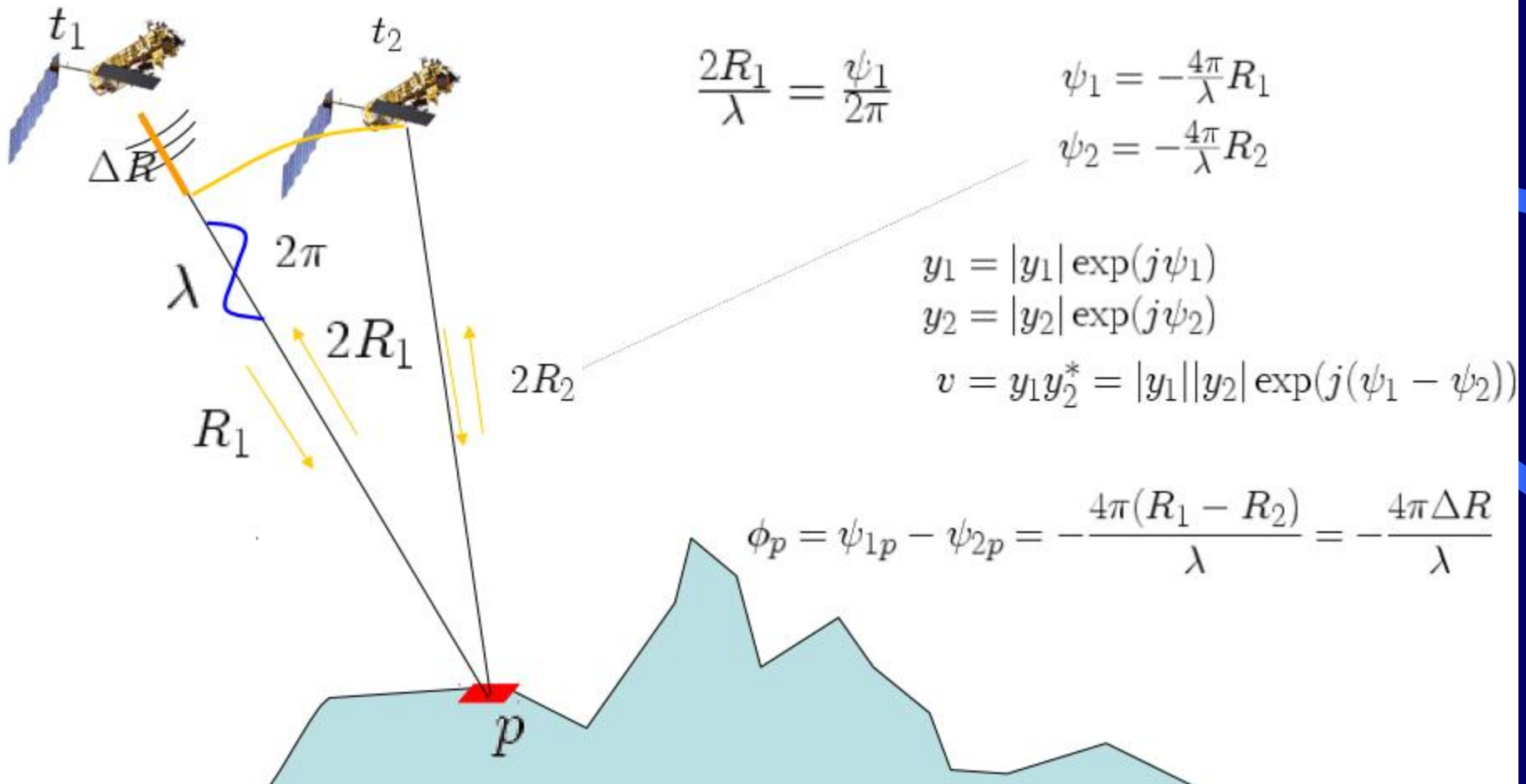


## Geometry of interferometry

Satellite orbit is very important for successful application of SAR interferometry. In general a normal baseline larger than 400m is usually not suitable for interferometry. Also baselines smaller than 40m may not be suitable for DEM generation but this data are very good for differential interferometry.

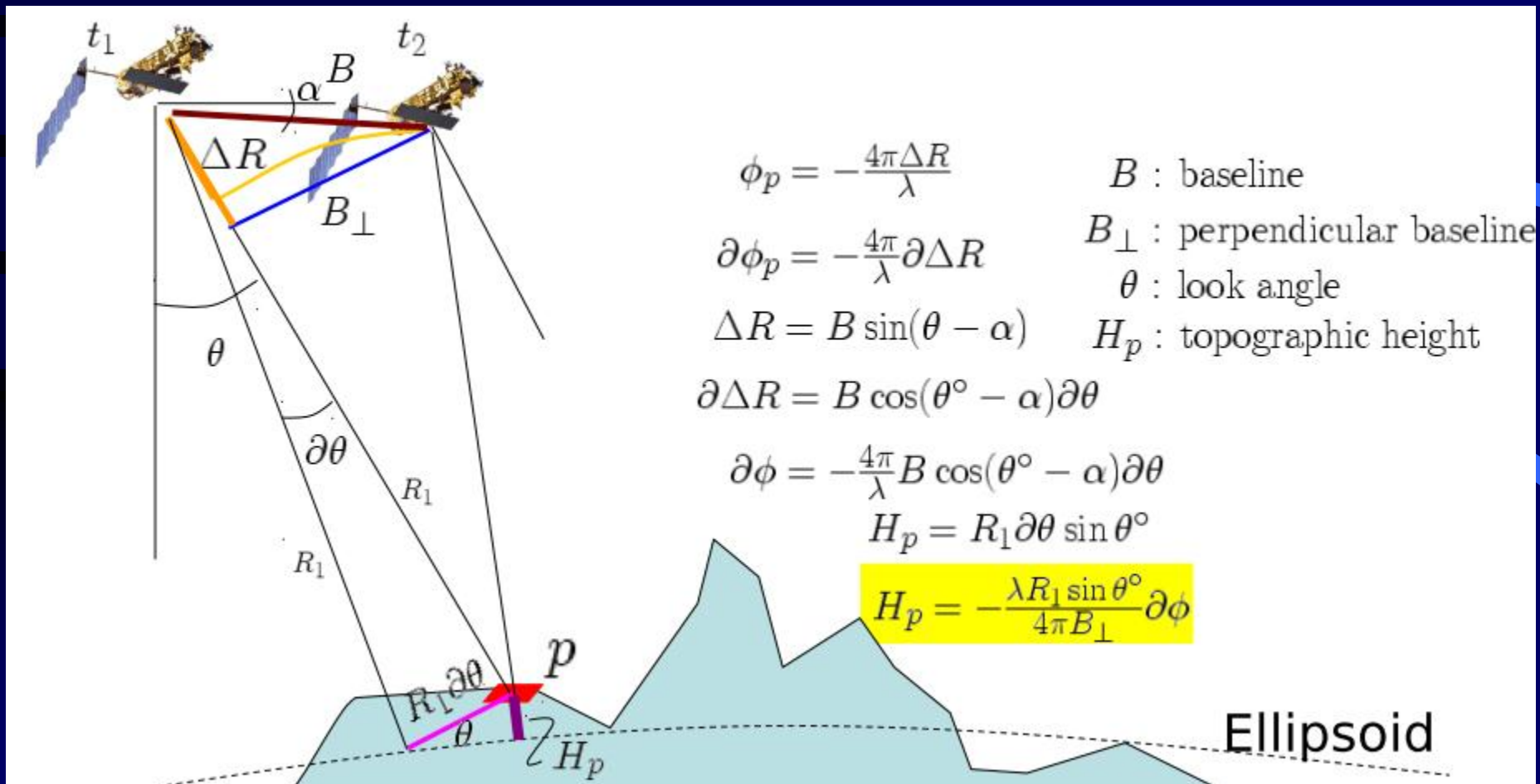


# Phase-range relationship



## Phase-height relationship

Topographic phase is inversely scaled by the perpendicular baseline.

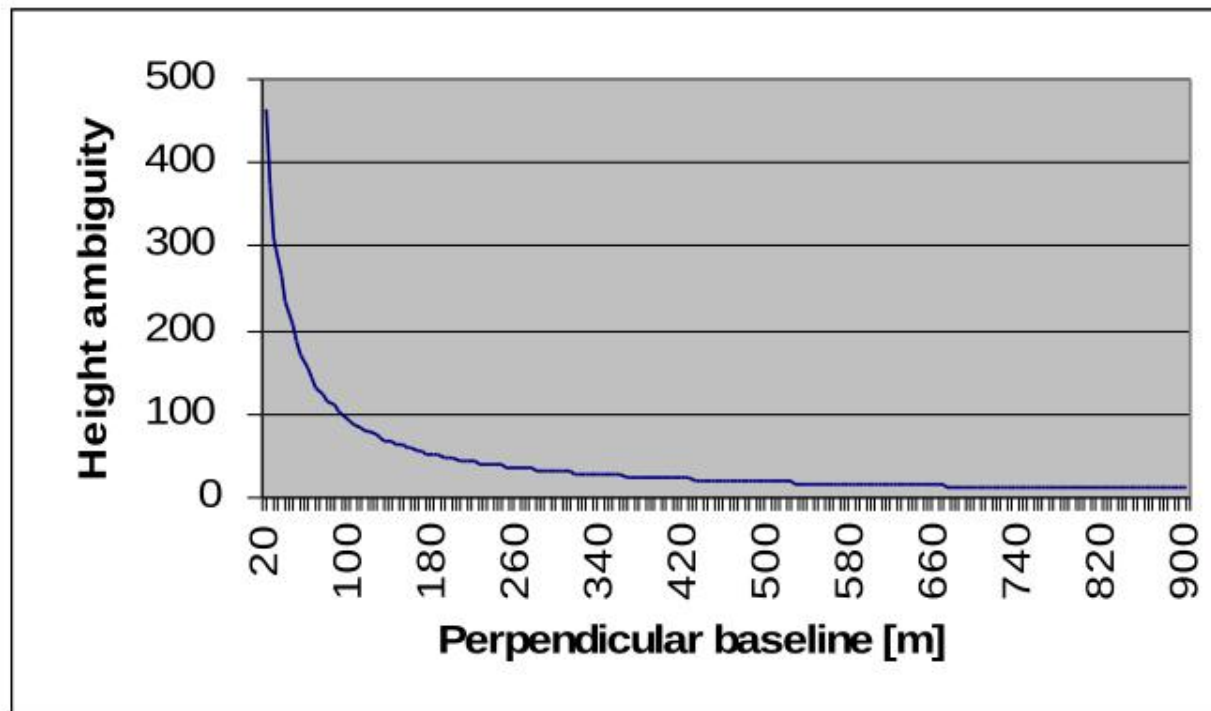


# Height ambiguity: sensitivity

**phase-to-height sensitivity:**

$$H_{2\pi} = \frac{-\lambda R_1 \sin \theta^\circ}{4\pi B_\perp} 2\pi = \frac{-\lambda R_1 \sin \theta^\circ}{2B_\perp}$$

**phase-to-height sensitivity:**



# Height ambiguity: sensitivity

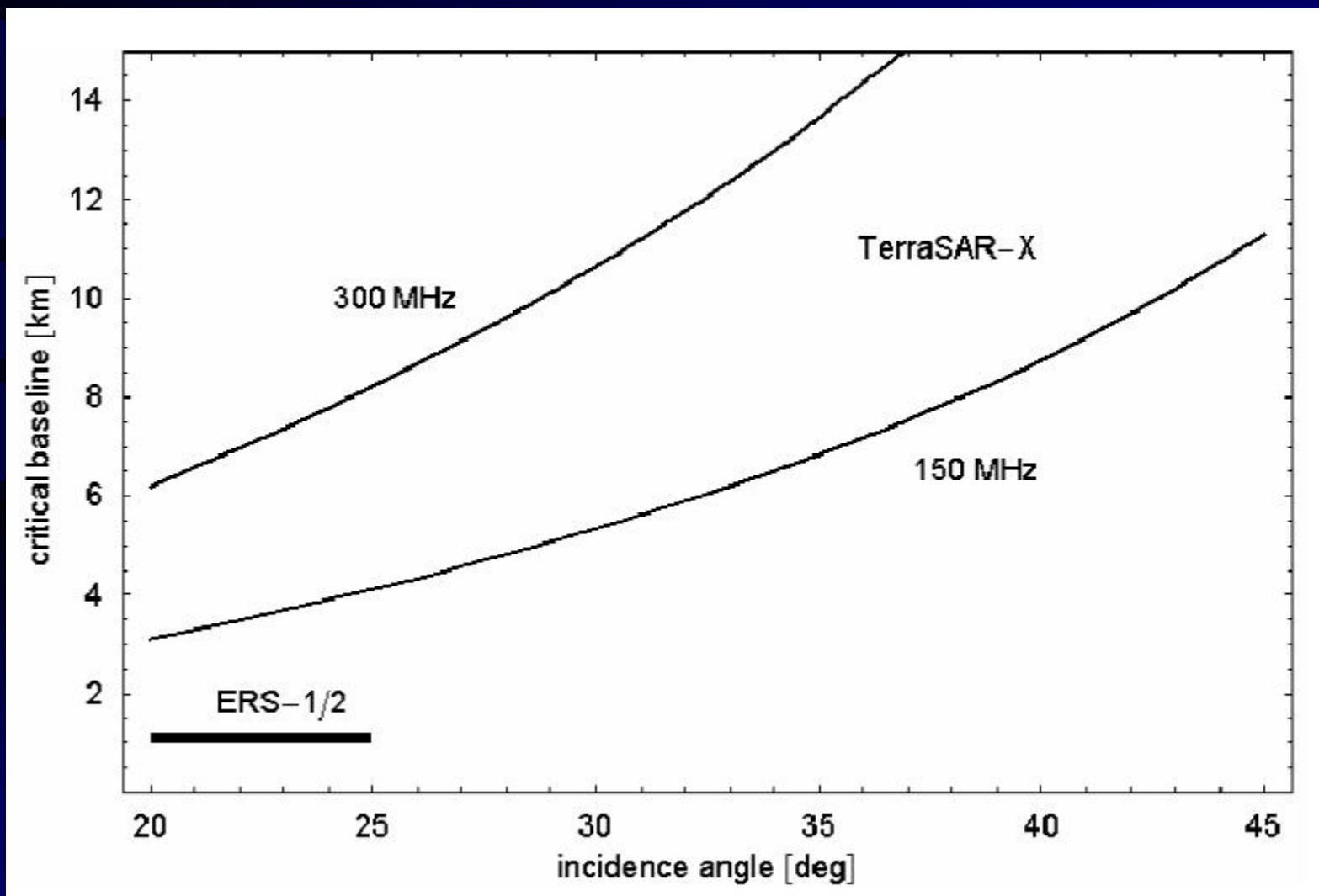
**Is there a limit to the baseline?**

**CRITICAL (=maximum) BASELINE**

$$B_{\perp, crit} = \left| \frac{W R \lambda \tan(\theta - \alpha)}{c} \right|$$

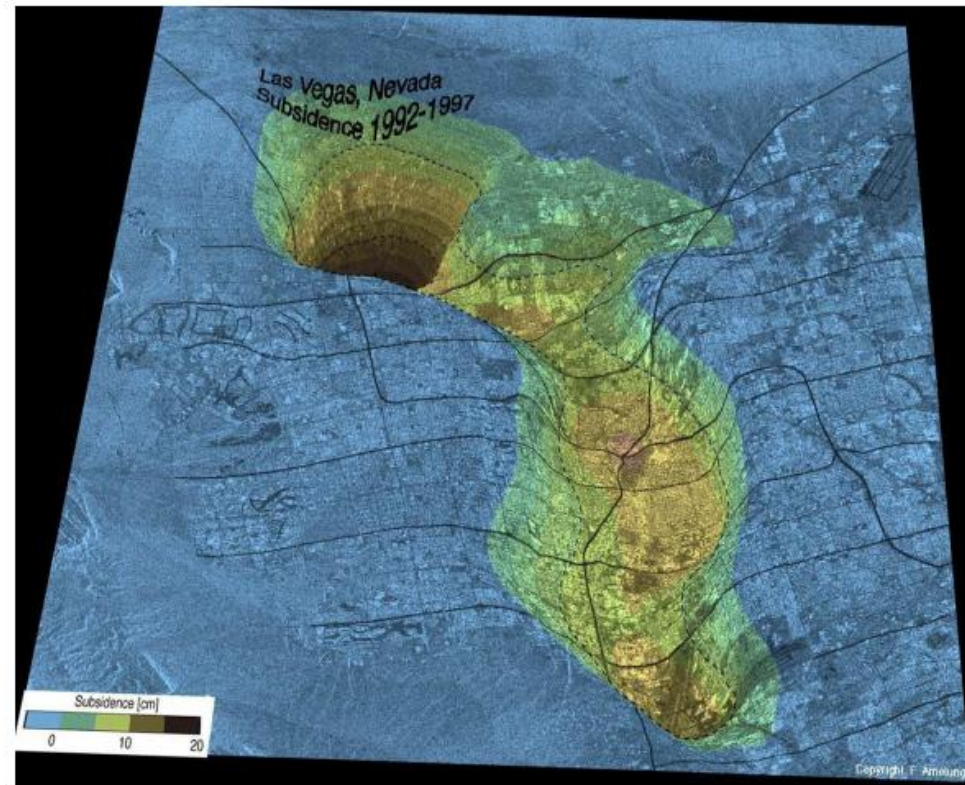
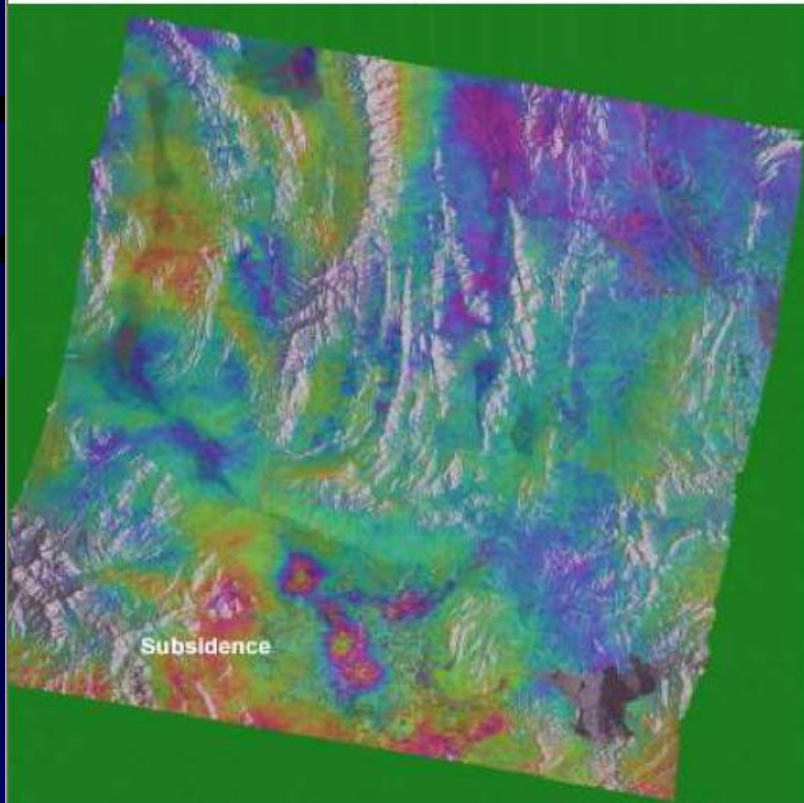
**$W$  : range signal bandwidth, for ERS: 15.5MHz**

# Critical baseline for ERS1/2 and TerraSAR X

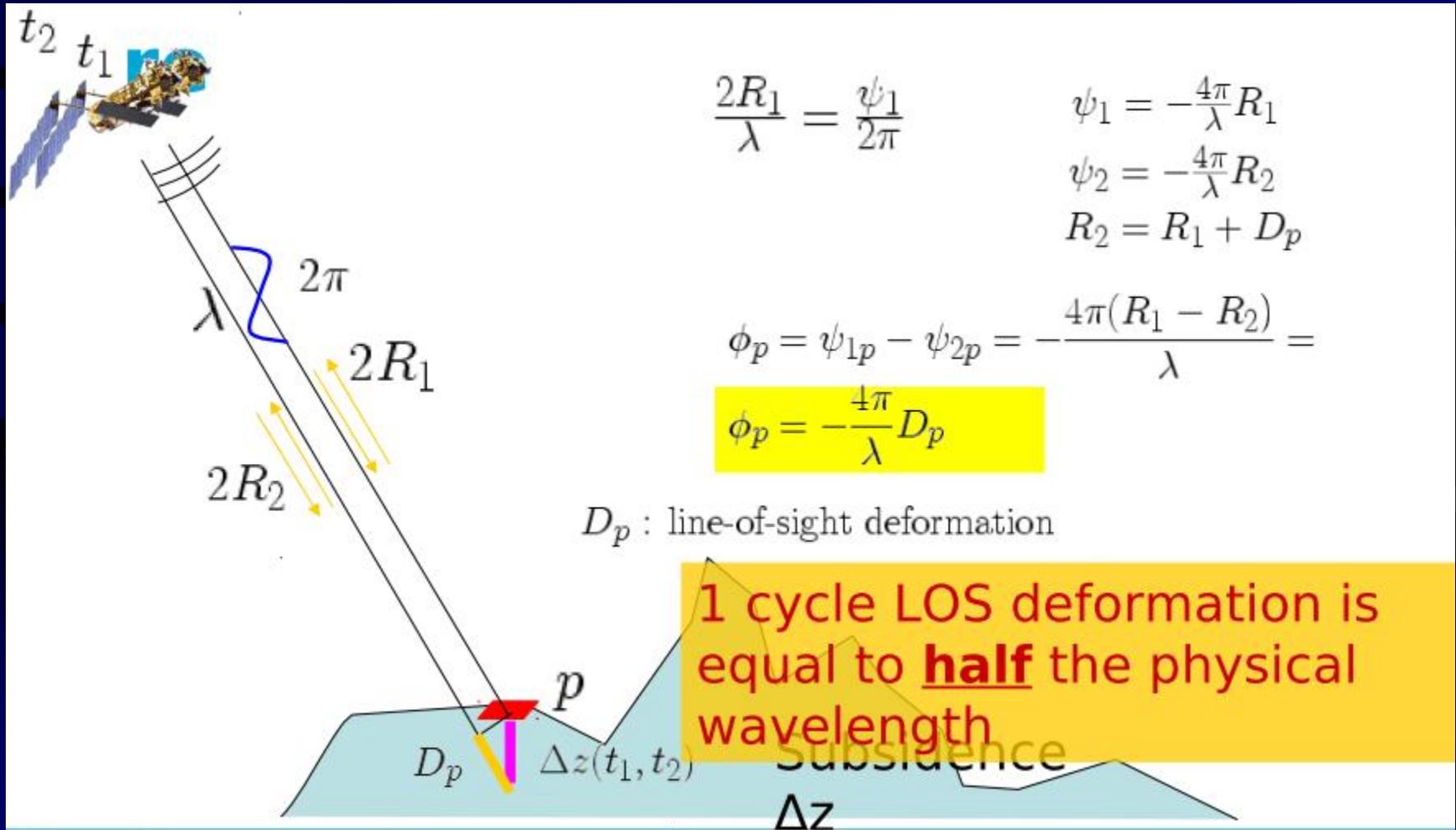


# Very sensitive to deformation

## Subsidence Las Vegas due to ground water

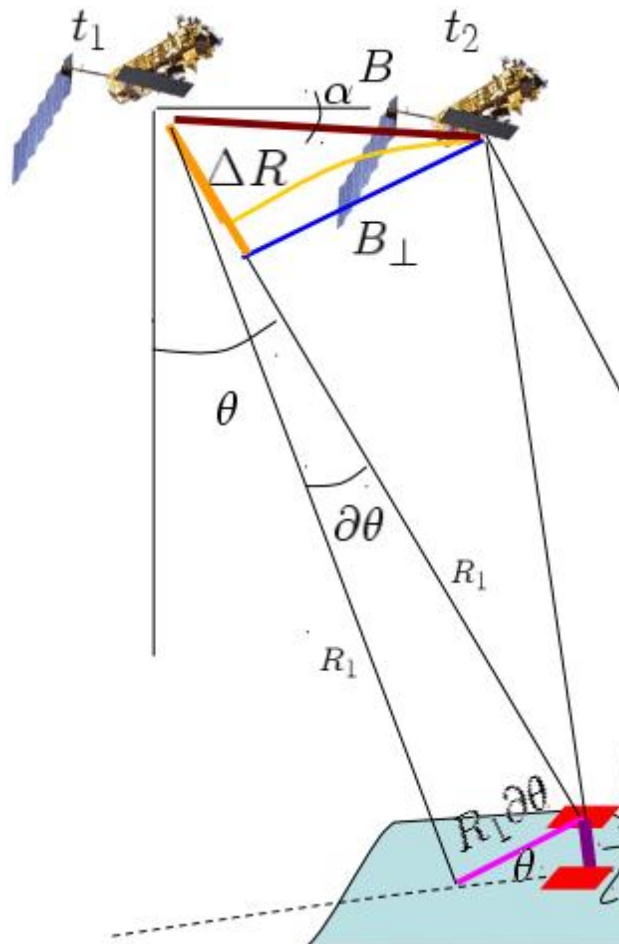


# Phase-deformation relationship





# Topography and deformation



$$H_p = -\frac{\lambda R_1 \sin \theta^\circ}{4\pi B_{\perp}} \partial\phi$$

$B$  : baseline

$B_{\perp}$  : perpendicular baseline

$$D_p = -\frac{\lambda}{4\pi} \partial\phi_p$$

$\theta$  : look angle

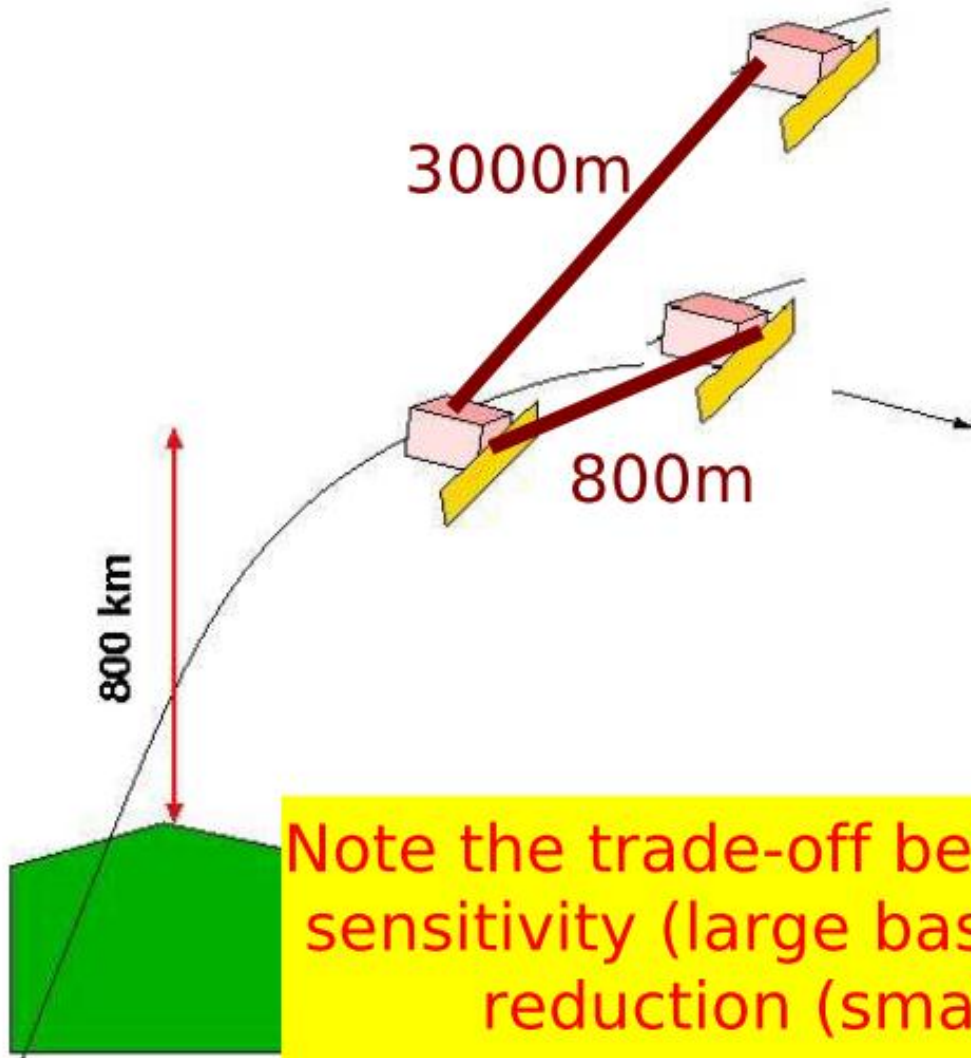
$H_p$  : topographic height

$$\partial\phi_p = -\frac{4\pi}{\lambda} \left( D_p + \frac{B_{\perp}}{R_1 \sin \theta^\circ} H_p \right)$$

Sensitivity to deformation  
1000x higher than for  
topography

Ellipsoid

# Geometrical correlation



- Baseline vary
- Relative scattering mechanism change
- Images become incomparable
- Function of baseline, doppler centroid, and terrain slopes

Note the trade-off between the height sensitivity (large baseline) and noise reduction (small baseline)

## Coherence estimation

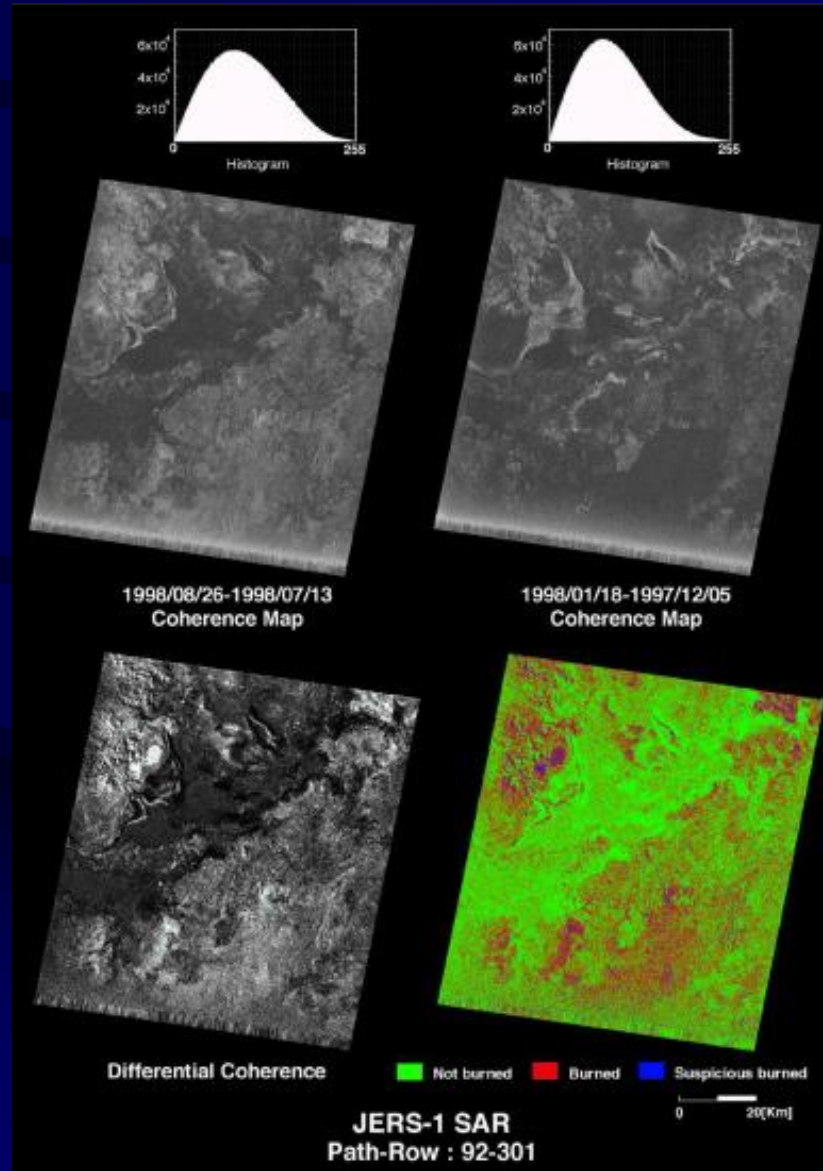
- Optics equivalent to correlation:

$$\gamma = \frac{E\{y_1 y_2^*\}}{\sqrt{E\{|y_1|^2\} \cdot E\{|y_2|^2\}}}$$

- Estimation of coherence:

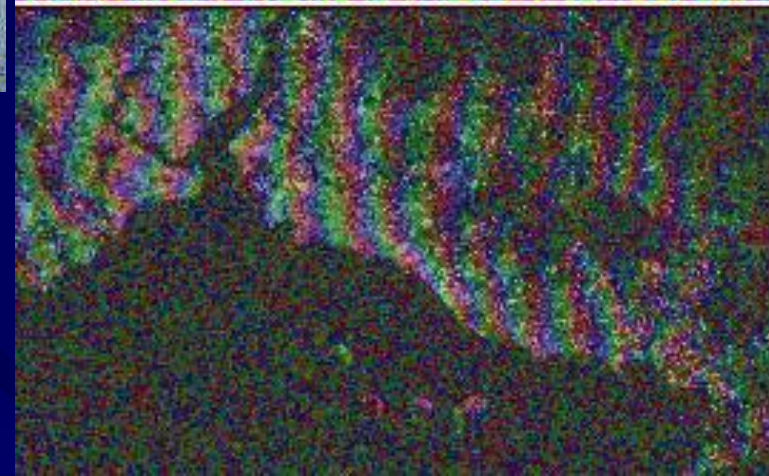
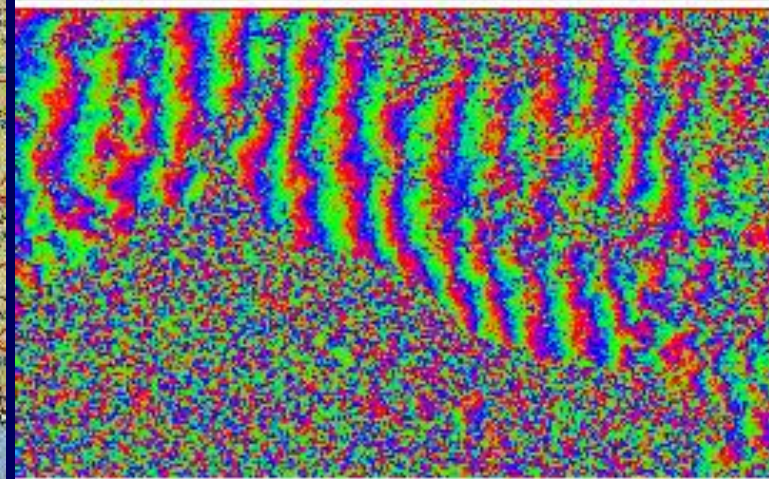
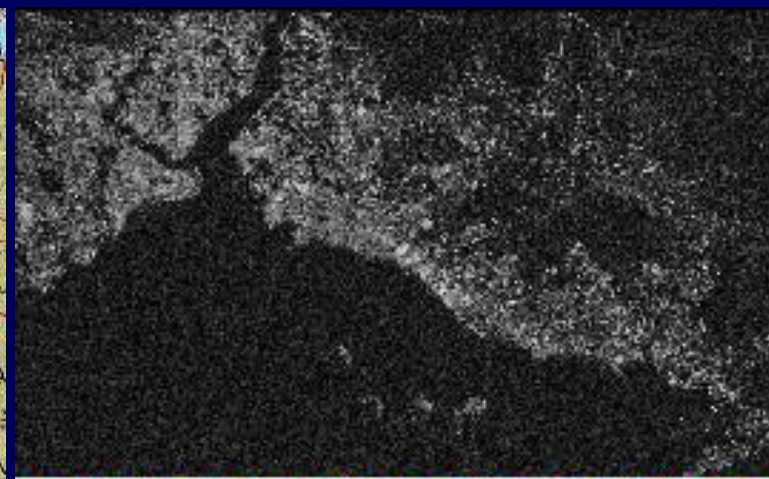
$$|\hat{\gamma}| = \frac{|\sum_{n=1}^N y_1^{(n)} y_2^{(n)}|}{\sqrt{\sum_{n=1}^N |y_1^{(n)}|^2 \sum_{n=1}^N |y_2^{(n)}|^2}}$$

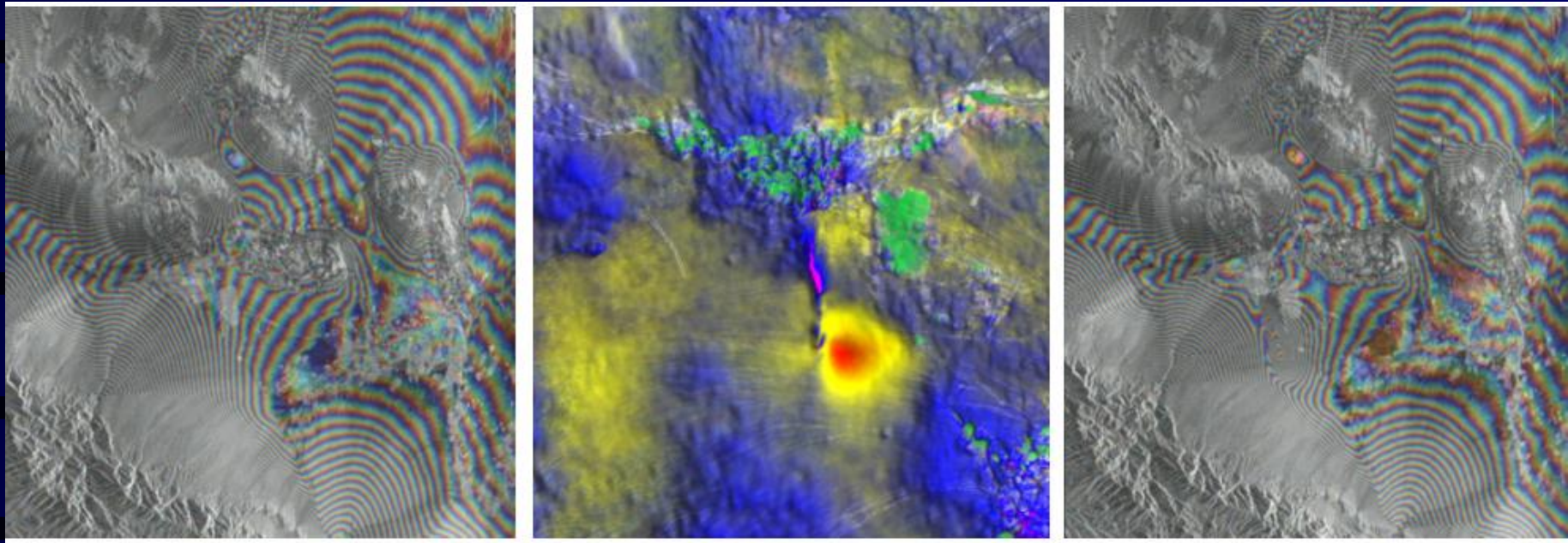
# Change detection



**New  
Technologies in  
monitoring and  
management of  
calamities and  
dynamic  
changes**

***Bosporus Strait***





**Left image: topo-DInSAR product of Envisat-ASAR data of 11 Jun and 3 Dec 2003  
(nbsl. 476.9m, pbsl. 141.6m)**

**Right image: topo-DInSAR product of the 3 Dec 2003 and 7 Jan 2004  
(nbsl. 521.9 m, pbsl. 268.3 m).**

**Middle image: 3-D perspective view of vertical displacement of south of Bam  
(during the 3.5 years after the 6.6 earthquake)**

**Displacements along the radar line-of-sight direction: 30 cm and 16 cm at south-east and north-east  
lobes of the interferogram**

**Displacement to the western part of the area, about 5cm along the radar line-of-sight direction**

# Thank you!

**KNOWLEDGE SHOULD BE SHARED,  
OTHERWISE IT IS USELESS.**

*ISNET can play a key role!*